



UNIVERSITY OF NAIROBI

**APPLICATION OF RAMAN SPECTROSCOPY IN COMPARATIVE
STUDY ON THE INFLUENCE OF IBUPROFEN AND *Asparagus racemosus*
(HERBAL EXTRACT) ON FEMALE REPRODUCTIVE HORMONES IN
WISTAR RATS**

BY

NAMANYA LOYCE

I56/11843/2018

**A Thesis Submitted for Examination in Partial Fulfilment of the
Requirements of the Award of Master of Science Degree in Physics of the
University of Nairobi.**

November 2020

DECLARATION

I declare that this thesis is my original work which has not been submitted anywhere for research and has been properly referenced and acknowledged following the requirements of the University of Nairobi.

Signature:



Date: 25/11/2020

Namanya Loyce

I56/11843/2018

Department of Physics

University of Nairobi

This thesis has been submitted with the approval of my supervisors

Signature

Date

Dr. Zephania Birech

Department of Physics,

University of Nairobi

P.O box 30197-00100, Nairobi Kenya. Email; birech@uonbi.ac.ke



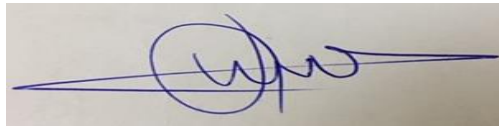
25/11/2020

Dr. Mureramanzi Silas

Department of Physics

University of Nairobi

P.O box 30197-00100, Nairobi Kenya. Email; mureramanzi@uonbi.ac.ke



25/11/2020.

Dr. Kaingu Catherine Kaluwa

Department of Veterinary Anatomy and Physiology

University of Nairobi,

P.O box 30197-00100, Nairobi Kenya. Email; ckaluwa@uonbi.ac.ke



25/11/2020

DEDICATION

I dedicate this report to my brothers and sisters to inspire them that anything is possible, the sky is no longer the limit.

ACKNOWLEDGMENT

First of all, I am so grateful to the all-powerful God by whose mercy and grace I have managed to learn, do research, and write this thesis.

I am so grateful to DAAD for the financial support I received from them that enabled me to pursue my post-graduate studies.

I truly acknowledge the valuable assistance with great gratitude my supervisors Dr. Zephania Birech, Dr. Mureramanzi Silas, and Dr. Kaingu Catherine Kaluwa have offered me. I have been able to work out successfully with their tireless effort, time, knowledge, ideas, advice, patience, and motivation.

With great appreciation, I thank Ms. Mwendu Kaaria Linet and Mr. Kwoba Daniel at the Department of Veterinary Physiology and Anatomy for agreeing to work with me and teaching me how to treat rats.

I extend my gratitude to the technicians Mr. Omucheni and Mr. Muthoka for the expertise and knowledge they have shared with me on how various equipment can be used while carrying out various tests and gathering data.

Special thanks to my classmates at the Department of Physics who shared with me their knowledge and also provided a comfortable learning atmosphere.

I thank my family (parents, siblings, and husband) and friends for their moral support and the opportunity to walk with me daily. I am so thankful for the endless prayers and best wishes.

ABSTRACT

Hormonal variation is a condition in which the body has less or more of a specific hormone which is a major cause of miscarriages, infertility, dysmenorrhea, breast cancer, among others in females. Measurements and detection of hormonal variation are currently achieved through the use of label-dependent and non-rapid methods such as Enzyme-Linked Immunosorbent Assay (ELISA), High-Performance Liquid Chromatography (HPLC), Gas Chromatography, and Mass spectroscopy. These methods are also expensive and involve complex sample preparation. In this work, the potentiality of the Raman spectroscopic technique in a comparative study on the influence of ibuprofen and *Asparagus racemosus* (herbal extract) on the levels of female reproductive hormones in the blood and vaginal fluid of Wistar rats is demonstrated. Portable Raman spectroscopic devices are also available and may be calibrated to perform hormonal level variation measurements. Here small volumes of blood samples (approximately 10 μL) obtained from the tail tip of the Wistar rats were applied onto conductive silver paint smeared microscope slides and Raman spectra measured upon 785 nm laser excitation. Raman spectra from the vaginal fluid of the same animals were also obtained. Using simulate samples consisting of blood from a male Wistar rat mixed separately with the four standard female hormones (Follicle Stimulating Hormone, FSH; Luteinizing hormone, LH; Progesterone and Estradiol) at different concentrations. The concentrations were within the ranges: (0.5 - 50 mlu/ml), (0.5 - 50 mlu/ml), (0.1 - 26.6 ng/ml), and (15 - 400 pg/ml) respectively. Using both ANOVA (Analysis Of Variance) and Principal Component Analysis (PCA) loadings plots, biomarker Raman bands of each of the hormones in blood were identified. The bands which exhibited significant intensity variation with concentration were centered at wavenumbers 1291 cm^{-1} for FSH, 682 cm^{-1} for estradiol, 1625 cm^{-1} for LH, and 1564 cm^{-1} for Progesterone. These bands were ascribed to CH_2 twisting vibration, $\text{C}=\text{C}$ stretching, CH_2 stretching, and $\text{C}=\text{C}$ stretching respectively. Using a chemometric data analysis tool (Artificial Neural Networks, ANN) on the Raman spectral data set, a model for each hormone was developed using the identified biomarker Raman bands, and the Limit of Detection (LOD) for each hormone estimated as 2.126 mlu/ml, 2.494 mlu/ml, 8.31×10^3 ng/ml and 8×10^{-3} pg/ml for FSH, LH, progesterone, and estradiol respectively. These LOD values were much lower than those reported for conventional detection techniques. The developed ANN models were also used to estimate the concentration levels of the respective hormones in blood samples obtained from untreated (normal), *Asparagus racemosus* (herbal extract) at low- (LD), and high-dose (HD), and ibuprofen

(IBU) treated Wistar rats. In general, it was found that compared to the untreated rats (Normal), administration of a high dose of *Asparagus racemosus* resulted in increased levels of FSH and estradiol by 5.2%, that of LH increased by 5% while that of progesterone increased by 5.2% in blood. Ibuprofen on the other hand was found to decrease the levels of FSH and LH by 5% and 4.9% and increase those of Progesterone and Estradiol by 5% and 5.1% respectively. The reproductive hormone level modification away from the normal are known to influence fertility hence from these results, administration of *Asparagus racemosus* and ibuprofen influence fertility. These results showed the great potential of Raman spectroscopy together with chemometrics in reproductive hormone level determination in blood. The work has also shown that the same Raman profiles of the treated and normal rats can be obtained by examining the vaginal fluid. Since the vaginal fluid is obtained non-invasively, this may be another interesting way to determine hormonal level variations. With proper calibration and validation, Raman spectroscopy can be used as a rapid (1 minute) hormone level screening tool in blood and vaginal fluid.

TABLE OF CONTENTS

DECLARATION	ii
DEDICATION	iii
ACKNOWLEDGMENT	iv
ABSTRACT	v
LIST OF TABLES	x
LIST OF FIGURES	xi
ABBREVIATIONS	xiii
CHAPTER ONE: INTRODUCTION	1
1.1 Background of the study	1
1.2 Statement of the Problem	5
1.3 Objectives of the study	6
1.3.1 Main objective	6
1.3.2 Specific objectives	6
1.4 Significance and Justification of the study	6
CHAPTER TWO: LITERATURE REVIEW	7
2.1 Chapter overview	7
2.2 Raman Spectroscopy as a detection technique	7
2.3 Conventional methods used in hormonal detection	9
2.3.1 Enzyme-Linked Immunosorbent Assay (ELISA)	9
2.3.2 High- Performance Liquid Chromatography (HPLC)	10
2.3.3 Electrophoresis	11
2.3.4 Mass spectrometry	12
2.4 Reproductive disorders associated with reproductive hormone level variation.	13
2.4.1 Dysmenorrhea (menstrual cramps)	13
2.5 Female Reproductive Hormones	14
2.6 Medication for Reproductive disorders	15

2.6.1 <i>Asparagus racemosus</i>	16
2.6.2 Ibuprofen.....	17
CHAPTER THREE: THEORETICAL FRAMEWORK	18
3.1 Chapter Overview.....	18
3.2 Raman spectroscopy.....	18
3.2.1 Raman setup and optimization.....	22
3.2.2 Assignment of Raman Peaks.....	23
3.3 Spectral Data Pre-processing.....	24
3.4 Chemometric Analysis Tools.....	25
3.4.1 Principal Component Analysis.....	25
3.4.2 Artificial Neural Networks.....	26
CHAPTER FOUR: MATERIALS AND METHODS	29
4.1 Chapter overview.....	29
4.2 Materials.....	29
4.3 Methods.....	30
4.3.1 Preparation of the Raman substrate.....	30
4.3.2 Sample preparation.....	32
4.3.3 Raman Spectroscopy Instrumentation.....	37
4.3.4 Optimization of Raman Spectrometric Measurements.....	39
4.4 Chemometric analysis of Raman spectra.....	41
4.4.1 Spectral data pre-processing.....	41
CHAPTER 5: RESULTS AND DISCUSSION	44
5.1 Characteristic Raman spectra of standard female reproductive hormones.....	44
5.2 Principal Component Analysis for Raman spectra of standard female reproductive hormones	45
5.3 Raman Spectra of standard female reproductive hormones mixed with Wistar rat's blood. .	47

5.4 Raman Spectra of blood samples obtained from normal (untreated), <i>Asparagus racemosus</i> (herbal extract), and ibuprofen treated female Wistar rats.....	53
5.5 Raman Spectra of vaginal fluid obtained from female Wistar rats treated with <i>Asparagus racemosus</i> (herbal extract) and ibuprofen.....	56
5.6 Quantification of hormones using Artificial Neural Networks (ANN).....	61
5.6.1 Quantification of the standard solutions of the female reproductive hormones mixed with male Wistar rat’s blood.....	61
5.6.2 Limit of Detection (LOD)	63
5.6.3 Quantification of the Raman Spectra of blood from normal(nontreated), <i>Asparagus racemosus</i>, and ibuprofen treated female Wistar rats.....	65
CHAPTER 6: CONCLUSION AND RECOMMENDATION	67
6.1 Conclusion	67
6.2 Recommendations	68
REFERENCES.....	69
APPENDICIES	79
APPENDIX 1: PCA Script in R.....	79
APPENDIX 2: ARTIFICIAL NEURAL NETWORK SCRIPT IN R.....	81
APPENDIX 3: Raman Spectroscopy set up at the Department of Physics, University of Nairobi	86

LIST OF TABLES

Table 2. 1: Advantages and disadvantages of conventional methods.....	11
Table 4. 1: Different concentrations of male Wistar rat's blood mixed with standard solutions of female reproductive hormones (Follicle Stimulating hormone FSH, Luteinizing hormone LH, Estradiol, and Progesterone).....	37
Table 4. 2: Laser power values at the different objective lens.....	40
Table 5. 1: Prominent Raman bands in Raman spectra of the standard hormones (LH, FSH, Progesterone, and Estradiol) when mixed with male Wistar rat's blood, the tentative component and vibrational assignment of the bands together with the references.....	49
Table 5. 2: Influence of Ibuprofen, normal Saline (control), and different doses of <i>Asparagus racemosus</i> on the female reproductive hormones in Wistar rats.	59
Table 5. 3: ANN validation results for each of the models developed for standard solutions of Follicle Stimulating Hormone, Luteinizing hormone, Progesterone, and Estradiol mixed with male Wistar rat's blood.....	62
Table 5. 4: Limit of Detection values in the Raman spectra of the standard hormones (LH, FSH, Progesterone, and Estradiol) when mixed with male Wistar rat's blood, literature values together with the references.	64
Table 5. 5: Concentration levels of the female reproductive hormone in the blood of days 3,7 and 11 for <i>Asparagus racemosus</i> treated, Ibuprofen treated, and the nontreated (normal saline) female Wistar rats.	65
Table 5. 6: Percentage deviation of <i>Asparagus racemosus</i> (herbal extract) and ibuprofen treated from the normal (untreated).	66

LIST OF FIGURES

Figure 3. 1: Diagram of Raman and Rayleigh Scattering (Moura et al., 2016).....	20
Figure 3. 2: A schematic diagram of the electronic and vibrational transitions for a diatomic molecule (Sato-berrú et al., 2004).....	21
Figure 3. 3: (a) A general dispersive Raman spectrometer (b) Fourier transform (FT) Raman spectrometer (Dzsaber et al., 2015).	23
Figure 3. 4: Schematic flow of ANN (Sensitivity and Trees, 2018).....	27
Figure 3. 5: (A) Diagram of an artificial neuron (B) Regression plot of obtained data and (C) Classification of the data collected on the sample (Zhelavskaya et al., 2018).	27
Figure 4. 1: Conductive Silver paste/paint.....	29
Figure 4. 2: Female Wistar rats stored in a cage.....	30
Figure 4. 3: Spreading of the conductive silver paste on the microscope glass slide.....	31
Figure 4. 4: Roots of <i>Asparagus racemosus</i> (herbal extract) after being washed.	32
Figure 4. 5: Powder form of <i>Asparagus racemosus</i> roots	33
Figure 4. 6: Ibuprofen tablets (Pharmacy in Nairobi Business Centre).....	34
Figure 4. 7: Blood samples being deposited on the microscope glass slide.	35
Figure 4. 8: Prepared blood samples ready to be studied with Raman Spectroscopy	36
Figure 4. 9: Basic Raman set-up of Raman schematic (Terchnotron Corp Raman Spectroscopy manual 2012)	38
Figure 4.10: Raman spectrum for the standard silicon wafer using 785 nm laser.....	39
Figure 4. 11: Raman spectrum before and after the use of Vancouver software.....	41
Figure 5. 1: Average characteristic Raman spectra of the female reproductive hormones standards Follicle Stimulating hormone, Luteinizing hormone, Estradiol and Progesterone with unique bands centered at 679, 1354, 1246, and 927 cm^{-1} respectively.....	44
Figure 5. 2: PCA 3D score plot of Raman spectral data set of the female reproductive standard hormones.....	46
Figure 5. 3: Loading plots together with Raman spectra of Luteinizing hormone, Follicle Stimulating Hormone, Progesterone, and Estradiol hormones.....	47

Figure 5. 4: Average characteristic Raman spectra of selected concentrations of female reproductive hormones standards FSH, LH, Estradiol, and Progesterone mixed with male Wistar rat’s blood. 48

Figure 5. 5: PCA 3D score plot of Raman spectral data set of (a) Estradiol, (b) Follicle Stimulating hormone, (c) Luteinizing hormone, and (d) Progesterone hormone mixed with male Wistar rat’s blood. 51

Figure 5. 6: Loadings plots together with Raman spectra of FSH, LH, Progesterone, and Estradiol hormone mixed with male Wistar rat’s blood..... 52

Figure 5. 7: Raman spectra of the blood samples for the untreated (normal saline), High and Low doses of *Asparagus racemosus* together with the Ibuprofen treated female Wistar rats on day 3, 7, and 11 with variance. 54

Figure 5. 8: Plots of Average intensity versus animal groups (treated and normal) for the selected days (Day 3,7 and 11). 55

Figure 5. 9:Raman spectra of the vaginal fluid samples for the nontreated (normal saline), High and Low doses of *Asparagus racemosus* together with the Ibuprofen treated female Wistar rats on day 3, 7, and 11 with variance. 57

Figure 5. 10: Plots of Average intensity versus animal groups (treated and normal) for the selected days (Day 3,7, and 11). 58

Figure 5. 11: ANN regression plots for Luteinizing Hormone, Follicle Stimulating Hormone, Estradiol, and Progesterone. 63

ABBREVIATIONS

ANOVA	Analysis of Variance
AR	<i>Asparagus racemosus</i>
CCD	Coupled Channel Detector
DNA	Deoxyribonucleic acid
EM	Electro Magnetic
EST	Estradiol
ET	Exposure Time
ELISA	Enzyme-Linked Immunosorbent Assay
FSH	Follicle Stimulating Hormone
FT	Fourier Transform
HD	High dose
HIV	Human Immune Virus
HPLC	High-Performance Liquid Chromatography
IR	Infrared
IBU	Ibuprofen
LD	Low dose
LH	Luteinizing Hormone
LSD	Laser Spot Diameter
LOD	Limit of Detection
MSE	Mean Absolute Error

ML	Machine Learning
mlu/ml	Milli-international units per milliliter
NA	Numerical Aperture
ng/ml	Nanograms per milliliter
NIR	Near Infrared
NRM	Normal
PCA	Principal Component Analysis
PC 1	1 st Principal Component
PC 2	2 nd Principal Component
PLS-DA	Partial Least Squares-Discriminant Analysis
Pg/ml	Picograms per milliliter
ppm	Parts per million
RRS	Resonance Raman Spectroscopy
REP	Relative error of prediction
RNA	Ribonucleic Acid
RMSE	Root Mean Squared Error
SERS	Surface-Enhanced Raman Spectroscopy
SD	Sprague Dawley
SNR	Signal to noise ratio
TERS	Tin Enhanced Raman Spectroscopy

CHAPTER ONE: INTRODUCTION

1.1 Background of the study

The use of Raman spectroscopy has significantly advanced since the last decade due to its analytical and potential diagnostic abilities. Raman Spectroscopy relies on the inelastic scattering of monochromatic light where photons lose or gain energy after interacting with molecules in a sample of interest (Raquel *et al.*, 2015). The resulting energy changes can be used to gain important information about the sample's molecular composition with a very high degree of precision. The obtained spectra contain molecular fingerprints of the Raman active components in the sample under study. The Raman signal emerges from radiative relaxations of vibrationally excited molecules. Since the energy structure is unique to each molecule, the spectral profiles of the Raman signals are also unique for each sample. Hence it provides a fingerprint of the components in the samples under study. Raman Spectroscopy is capable of distinguishing different samples based on the sample composition and molecular vibrations (Raquel *et al.*, 2015).

Raman spectroscopy can study molecules in special nano-resonators where their efficiency in light scattering is so high such that a limit of detection (LOD) of up to the order of 10^{-18} mol dm^{-3} can be achieved (Kudelski, 2008). This technique has also been widely incorporated in biological, medical, food science, environmental, and industrial sample analysis (Craig *et al.*, 2013, Zavaleta *et al.*, 2009). In most of these cases, it is mainly used to identify molecules or compounds in a sample and even define the distribution (Raquel *et al.*, 2015).

Raman spectroscopic technique has been applied in the study of blood from Sprague Dawley rats to detect diabetic ones from those that are healthy (Birech *et al.*, 2017), in the diagnosis of various cancers like cervical, ovarian, prostate, and breast cancers giving detailed molecular data of the cells (Auner *et al.*, 2018) and in the screening of the Human Immune Virus (Otange *et al.*, 2017).

In this work, the Raman spectroscopy technique was explored for hormonal variation detection in blood and vaginal fluid of Wistar rats that were administered ibuprofen and *Asparagus racemosus* (herbal extract). These were compared with those administered normal salines as a control group. The advantages of using this technique include:

- 1) Minimal sample preparation is required
- 2) Small samples can be studied since the laser beam can be focused on a tight spot.
- 3) Insensitivity to water hence aqueous samples can be studied.

- 4) Excellent specificity
- 5) It is not time-consuming.
- 6) Relatively affordable as compared to the detection techniques available.

By the time of preparing this thesis, there was no published study that we came across reporting on Raman Spectroscopic detection of hormonal variation in blood and vaginal fluids of rats or any animal treated with *Asparagus racemosus* (herbal extract) and ibuprofen. However, related research has been done on the application of Raman spectroscopy on screening cervical cancer based on hormonal variation (Duraipandian *et al.*, 2012).

Various techniques that are currently used to detect hormonal variation include the Enzyme-Linked Immunosorbent Assay (ELISA), Mass spectroscopy, Electrophoresis, and High-Performance Liquid Chromatography (HPLC) (Vance *et al.*, 2016a, Colah *et al.*, 2007). ELISA is a convectional detection method that measures antigen concentration through the detection of interference in the signal. Two antigens are required for any measurement to be taken and that is the sample antigen and the reference antigen. The sample antigen is bound on the reference antigen to be able to carry out the detection process. ELISA is easy to perform and very sensitive though sample preparation is complex, it is limited to antigen information, produces low signal information, and is very expensive (Vance *et al.*, 2016a).

High-Performance Liquid Chromatography uses high pressure to analyze and isolate samples from a mixture or compound depending on the chemical structure and composition. HPLC uses a variety of quantities in very small quantities for any detection to be done (Jebaliya *et al.*, 2013). This technique is sensitive and performs both qualitative and quantitative analysis but complex, expensive, equipment requires timely maintenance and produces noisy data (Colah *et al.*, 2007).

Electrophoresis is a technique hinged on the migration of charged molecules in an electric field applied at different speeds. The sample for analysis must be protein in nature like hormones, enzymes, antibodies, and nucleotides (RNA and DNA). This is a quantitative and qualitative analysis technique that operates on the principle of separation, very sensitive but time consuming, bulky, and expensive (Reddy and Raju, 2012).

Mass spectrometry is an analytical technique that determines the molecular formula, weight, structure, protein sequence, and isotopic distribution in the sample under study. The process of mass spectrometry involves four stages in the order of Ionisation, Acceleration, Deflection, and Detection (Aretz and Meierhofer, 2016).

The technique has been demonstrated in understanding biological systems like enzymes, antibodies, hormones. The mass spectroscopic technique is fast and requires small sample sizes though very expensive, does not give structural information directly, and requires a lot of sample preparation (Hale, 2013).

Hormonal variation detection is very important because it plays a great role in the general health of the reproductive system and is also a great determinant of fertility. Hormonal variation is a disorder arising when there is less or more of a given hormone in the body (Naveed *et al.*, 2015). Hormones are chemical transmitters produced by the endocrine glands that are responsible for body system development. Different hormones are responsible for the growth, repair, reproduction, and development of different body systems like the reproductive system, nervous system among others (Jansson *et al.*, 2008). These hormones include glucagon, reproductive hormones, growth hormone, oxytocin, prolactin, thyroid-stimulating hormone among others (Jansson *et al.*, 2008).

Reproductive hormones have a central role in the reproductive system's growth, development, and functioning. There are various hormones in the reproductive system responsible for the male and female reproductive systems. The testosterone hormone is in charge of the male reproductive system (Stellato *et al.*, 2000). And those in charge of the reproductive system in females are estradiol, follicle-stimulating hormone, progesterone, and luteinizing hormone (Christensen *et al.*, 2012a). Hormonal variability in the sex hormones is typically noticeable in the female reproductive system during ovulation and menstruation period due to body changes and development.

In Wistar rats, the oestrus cycle is known to be the reproductive cycle and it is usually 4 to 5 days while in humans it is the menstrual cycle that is usually 21 to 30 days. The oestrus cycle has four different stages that are proestrus, estrus, metestrus, and diestrus. Female reproductive hormones are responsible for the reproductive cycle and each hormone plays a different role (Caligioni, 2009).

Estradiol hormone is developed in the ovary by follicles and plays a key role in the rapid growth of uterine endometrial cells hence controlling the menstrual cycle (Caligioni, 2009).

Progesterone hormone is produced by the corpus luteum a steroid gland found in the ovary and is responsible for maintaining the uterus lining in preparation for implantation and also keeping the pregnancy (Caligioni, 2009). Follicle Stimulating Hormone stimulates folliculogenesis and oogenesis resulting in the release of the ovum into the oviduct (Caligioni, 2009). Luteinizing hormone works closely with FSH in estradiol synthesis by ovarian granulosa cells and also triggers ovulation (Caligioni, 2009).

Reproduction is a process that occurs when there is harmonious functioning of the nervous system and the peripheral organs which are achieved by the hypothalamic-pituitary-gonadal axis in charge of proper coordination of ovulation with the reproductive system. Ovulation is the release of the ovum from the ovary (Christensen *et al.*, 2012b).

The female reproductive system's functionality is determined by the reproductive hormones; they are a great determinant of female fertility, reproduction, proper functionality, and development of the female reproductive system processes like puberty, ovulation, implantation, and other reproductive processes (August *et al.*, 2017).

Drugs administered for the management of menstrual pains (Dysmenorrhea) and other reproductive disorders like infertility are believed to have some influence on the variation of the reproductive hormones during the treatment of these disorders (Jashni *et al.*, 2016). Dysmenorrhea affects the life of women negatively if not properly managed. Menstrual pains are cramp-like pulsating pains that are usually experienced by most of the women in their lower abdomen during or before menstruation for a period of one to four days (Grandi *et al.*, 2012). Menstrual pains result from the contraction of the uterus (shedding off of the uterus walls). This pain in some women is mild while in others it is severe. Pain relief medications like paracetamol, ibuprofen, naproxen sodium, and natural herbs like *Asparagus racemosus* and *Pipe guineense* are administered to manage menstrual pains and other reproductive disorder (Kaaria *et al.*, 2019).

In this study, two drugs were administered to female Wistar rats; ibuprofen and *Asparagus racemosus* (high and low dose), and blood and the vaginal fluid samples are obtained from them investigated with Raman spectroscopy. The blood was drawn from the tail tip of the rats after making a simple cut then squeezed onto the conductive silver smeared microscope glass slides. They were then excited using a 785 nm laser after air drying and Raman spectra recorded and analyzed. Vaginal fluid drawn from the same rats using a pipette was also applied onto the same Raman substrates and Raman measurements were done similarly.

The spectral data obtained using Raman Spectroscopy suffers fluorescence and noise. This data is also hard to interpret because it is multidimensional making it hard to extract the desired information. Multivariate chemometric methods like Artificial Neural Networks (ANN), Principal Component Analysis (PCA) were employed to overcome these limitations. Multivariate chemometric methods become handy in reducing the complexity of the data acquired (Hanson, 2012). PCA and ANN chemometric analytical tools were applied for data visualization, characterization, and extraction of the most important and required sample information from the Raman spectral data set as large data are collected.

ANN is normally used to extract quantitative information on multivariate spectral data and can also be used in regression analysis (Wu and Massart, 1996), and PCA on the other hand is handy in the reduction of the dimensions of the spectral data through clustering (Ullah *et al.*, 2019).

This thesis is made up of six (6) chapters. In chapter one we have the introduction, statement of the problem, Objectives, Significance, and justification of the study. Chapter two gives the related literature to the study; chapter three discusses the theoretical framework of the Raman spectroscopic technique and Chemometric analysis tools. In chapter four, the materials and methods used to carry out the research are explained, chapter five is about Results and discussion and the last chapter gives the conclusion on the results obtained, the technique used, and recommendations for further research and study.

1.2 Statement of the Problem

Hormonal variation if not identified and treated early results in serious reproductive disorders like miscarriage, infertility, breast cancer that cause malfunctioning of the female reproductive system. Currently, the available conventional hormonal variation detection techniques (ELISA (hormonal kits), HPLC) are expensive, time-consuming, require tedious sample preparation procedures, are label-dependent, complex, and do not yield immediate results.

The Raman spectroscopy coupled with multivariate chemometric techniques showed the potential to overcome these shortcomings and provide a better diagnosis and analytical tool for hormonal variation detection in blood since it is sensitive, fast, able to provide instant results, involves less sample preparation, and has excellent specificity.

1.3 Objectives of the study

1.3.1 Main objective

The main objective of this study is to explore the potential of Raman spectroscopy in a comparative study on the influence of ibuprofen and *Asparagus racemosus* (herbal extract) on female reproductive hormones in the blood and vaginal fluid of Wistar rats.

1.3.2 Specific objectives

- 1) To measure and analyze Raman spectra from blood from female Wistar rats treated with *Asparagus racemosus* (herbal extract) and ibuprofen, and the non-treated ones.
- 2) To measure and analyze Raman spectra from the vaginal fluid of the rats in objective (1).
- 3) To obtain characteristic Raman spectra of Standard solutions of female reproductive hormones (progesterone, follicle-stimulating hormone, estradiol, and luteinizing hormone).
- 4) To use chemometrics tools (PCA and ANN) in segregating and quantifying the Raman spectral data obtained.

1.4 Significance and Justification of the study

The conventional detection methods have for decades been the great methods for detection and diagnosis because they are sensitive and able to give both qualitative and quantitative results on hormonal variation detection. Despite their detection accuracy, there are more serious backdrops that include being more costly, time-consuming, and requiring too much sample preparation. This means that the conventional detection methods remain a challenge.

Raman Spectroscopic technique coupled with chemometrics in the detection of hormonal variation in blood and vaginal fluid of the female Wistar rats has the potential to overcome the challenges being faced with the conventional detection methods and hence revolutionizing fertility studies in humans since the rats' reproductive system has similarities to that of humans (Sengupta, 2013). Also, the fact that small samples are needed together with the rapidity of results delivery makes Raman spectroscopy a better tool in the quick screening of a large population.

CHAPTER TWO: LITERATURE REVIEW

2.1 Chapter overview

In this chapter, a review of Raman spectroscopy as a detection technique and different available conventional methods that have been employed in the diagnosis of hormonal variation are reviewed. The chapter also covers the female reproductive system, the hormones responsible for its development and functioning, reproductive disorders, and medication

2.2 Raman Spectroscopy as a detection technique

For the last decade, the use of Raman Spectroscopy has greatly and significantly advanced in various detection fields and this has become an interesting area of research because of its analytical capabilities. This technique has been extended to different fields for the detection and analysis of variations to study their detailed composition due to its sensitivity property. Raman Spectroscopy has several uses in different scientific fields such as Physics, Biochemistry, Clinical Microbiology, Food Science, Biology because of its strong and smart spectroscopic capability (Craig *et al.*, 2013, Zavaleta *et al.*, 2009). Raman spectroscopy can give a detailed material fingerprint of biofluids, molecules, tissues, and cells giving their specific features and detailed chemical composition (Raquel *et al.*, 2015). Raman Spectroscopy is also able to give the quantitative information of the sample of interest concerning in terms of its chemical composition (Kong *et al.*, 2015).

In many applications, the Raman technique is very flexible and molecular precise. Raman Spectroscopy obtains spectral profiles with peaks and valleys revealing various samples' rotational and vibrational transitions (Kong *et al.*, 2015). The spectral profiles provide precise and distinctive sample information of the sample under study. The spectrum is an intensity-wavenumber or wave shift (cm^{-1}) plot.

Raman spectroscopy has been explored in the study of the effect of hormonal variation on cervical cancer detection (Kanter *et al.*, 2009) and also on the use of high wave numbers in pre cervical cancer detection (Duraipandian *et al.*, 2012). The results showed significant variations at peaks centered at 2924 and (3100-3700) cm^{-1} when the data of the normal and patients were compared.

Raman spectroscopy was used to measure levels of glucose in Sprague Dawley rats' blood for which anti-diabetic medication and medicinal plants were administered (Birech *et al.*, 2017).

The differences in the Raman intensity of the spectral profiles suggested different glucose levels in the analysis of blood samples. This detection method has also become a basic instrument for the diagnosis and imaging of prostate, pancreatic, and ovarian cancer (Auner *et al.*, 2018). Ovarian cancer was detected at Raman bands centered at 718, 1004, 1247, 1090, 1321, 1340, 1440, and 1660 cm^{-1} that showed variations of proteins and lipids in the ovary and fallopian tubes (Auner *et al.*, 2018).

Raman spectroscopy has been reported to have the potentiality of monitoring pregnancy changes where preterm labor was detected (Vargis *et al.*, 2011). This was important since preterm labor is recognized as among the causes of neonatal mortality, delayed development, and cerebral palsy (Vargis *et al.*, 2011). In this study, Raman shifts showed differences by calculating the *p*-value for the data collected. With the Raman shifts, changes were also noticed with cervical softening and hormonal variation (Vargis *et al.*, 2011).

Scientists have applied Surface-Enhanced Resonance Raman Scattering (SERRS) to analyze differences in sex hormones, such as estrogen other than the conventional detection methods (Vedad *et al.*, 2018). With Raman Spectroscopy, the forms of estrogen (estradiol (E2), estriol (E3), estrone (E1), and ethynlestradiol (EE2)) were differentiated and quantified. The Raman bands for each were identified; 546 cm^{-1} for E2, 581 cm^{-1} for E1, 597 cm^{-1} for EE2 and 762 cm^{-1} for E3 (Vedad *et al.*, 2018).

Raman Spectroscopy technique was explored in the identification of single bacteria and demonstrated that even the smallest single bacterial cells can be probed (Strola *et al.*, 2014). The technique of Surface Enhanced Raman Spectroscopy demonstrated the ability to single out *Bacillus anthracis* from a family of 27 strains of *Bacillus* (Strola *et al.*, 2014).

The potentiality of the Raman Spectroscopy has been demonstrated in the determination of the composition of the brain tissue when reduced graphene oxide is administered (Mendonca *et al.*, 2015). This study was carried out on rats that were injected with reduced graphene oxide (Soares *et al.*, 2016). Raman Spectroscopy demonstrated alterations in chromatin patterns and neuronal nuclear membranes hence proving to be a great technique in evaluating molecular effects due to nanomaterials (Soares *et al.*, 2016).

The technique of the Raman Spectroscopy has also been used in the chemical analysis of different chemical compounds hence an analytical tool that is non-destructive and very ideal for the characterization of different white substances obtained from forensic and archaeological burial contents (Schotsmans *et al.*, 2014).

Surface-Enhanced Raman Spectroscopy (SERS) works on the same principle as normal Raman Spectroscopy but with a greatly enhanced signal. SERS has a very high spatial resolution and is so sensitive for detection (Zhang *et al.*, 2005). Different metals like silver, gold, and copper are used as substrates because they contain metallic nanoparticles that have high conductivity (Corio *et al.*, 2002, Faulds *et al.*, 2002). SERS uses nanostructures that are metallic and can enhance weak signals.

During enhancement, there is adsorption of molecules that have a structure close or similar to that of the metallic nanostructure which enables interaction of the excited surface plasmons with light during resonant interaction. An enhanced electric field of approximately 10^2 is created due to resonant interaction in the region around the surface (Kong *et al.*, 2015). Enhancement is achieved when there is an adsorption of molecules onto the surface of the metallic nanostructures.

This research investigates the Raman Spectroscopy technique in the detection of hormonal variation in female reproductive hormones; Estradiol, progesterone, Follicle Stimulating Hormone, and Luteinizing hormone of Wistar female rats to which various doses of *Asparagus racemosus* and ibuprofen have been administered for fourteen days.

Despite the advantages of using the Raman spectroscopic technique that includes being fast, highly sensitive, having excellent specificity, and requiring less sample preparation, it cannot be used to interpret and process the data collected and therefore chemometric analysis techniques such as the Principal Component Analysis (PCA), Artificial Neural Networks (ANN) have to be applied to extract the required information from the large data set collected.

2.3 Conventional methods used in hormonal detection

Various methods have been applied in hormonal variation detection which includes; Enzyme-Linked Immunosorbent Assay (ELISA), Mass spectrometry, electrophoresis, and High-Performance Liquid Chromatography (HPLC).

2.3.1 Enzyme-Linked Immunosorbent Assay (ELISA)

This detection technique is very sensitive and depends on Monoclonal antibodies which are man-made protein in nature. The use of ELISA involves the following procedures: reference antigen coating, the addition of specific antigen to be measured which is usually a sample under study, addition of the secondary antigen which is enzyme-conjugated, addition of substrate and then incubation of 12 to 48 hours before taking any measurement (August *et al.*, 2017).

ELISA has been applied in the determination of food authenticity for foods like meats, fishery products, fruits, and dairy products which is very fundamental in value assessment (Asensio *et al.*, 2008). Meats from different animal species were identified, dairy products like milk and cheese were classified differently. Milk from different animals like cows and goats was also differentiated (Asensio *et al.*, 2008).

ELISA has also been applied in various fields like vaccine development, pharmaceutical industries, infectious diagnosis, transplantation, toxicology to mention but a few (Hosseini *et al.*, 2018).

With ELISA, pesticides like atrazine one of the most commonly used pesticide in the world and is known to have endocrine-disrupting effects were detected. Different matrices were used for the detection of this pesticide but a quick response was obtained when in water (Gascon *et al.*, 1997).

ELISA has been applied in the detection of progesterone one of the female reproductive hormones and was able to detect concentrations that are as low as 0.2 ng/ml (Khatun *et al.*, 2009).

2.3.2 High- Performance Liquid Chromatography (HPLC)

This is another technique with various applications in analysis, detection, quantification in biomedical fields. This method involves separating compounds in the mixture and this is possible because compounds have different affinities.

HPLC has been applied in the detection of estradiol (E2), ethynylestradiol (EE2), and bisphenol A (BPA) in urine samples of humans, and the concentrations ranging from 20 to 42 pg/ml were detected (Kumar *et al.*, 2014).

HPLC has also been applied to detect Luteinizing hormone and Follicle-stimulating hormone levels in human serum and concentrations as low as 0.005 lu/l for LH and 0.010 lu/l for FSH were detected (Robertson *et al.*, 2001).

The compounds of the same chemical composition and structure are isolated. The advantages and disadvantages of these conventional methods are summarized in table 2.1 below.

Table 2. 1: Advantages and disadvantages of conventional methods

Conventional methods	Advantages	Disadvantages	References
High-Performance Liquid Chromatography (HPLC)	Able to perform a quantitative and qualitative analysis	Very expensive since HPLC instrumentation uses expensive solvents	(Colah <i>et al.</i> , 2007)
	Very sensitive and able to detect very small concentrations of substances	Sample preparation is complex, it involves mixing, homogenization, filtration, and degassing.	
		Time-consuming	
		Produces non-homogeneous and noisy data	
		Equipment requires timely maintenance.	
Enzyme-Linked Immunosorbent Assay (ELISA)	Easy to perform	Has low signal amplification	(Vance <i>et al.</i> , 2016b)
	Very sensitive	Limited to antigen information.	
		Detection is based on enzyme reactions so results are obtained in a short time	
		Requires too much sample preparation	

2.3.3 Electrophoresis

This is a technique hinged on the migration of charged molecules in an electric field applied at different speeds. This is a quantitative and qualitative analysis technique that operates on the principle of separation. The sample for analysis must be protein in nature like hormones, enzymes, antibodies, and nucleotides (RNA and DNA).

This technique has been applied in biomedical research, microbiology, biochemistry, medical detection, and analysis among others (Reddy and Raju, 2012).

Electrophoresis coupled with ion-pair hollow fiber liquid to liquid microextraction in the detection of thyroid hormones in human serum samples yielded good results in differentiating the four thyroid hormones (3,5-diiodo-L-thyronine dihydrate (T_2), 3,5,3-triiodo-L-thyronine (T_3), reverse 3,3,5-triiodo-L-thyronine (rT_3), and L-thyroxine (T_4)) (Li *et al.*, 2014).

Electrophoresis has been applied to detect any presence of Luteinizing hormone in brain neuropeptides from ewe median eminence. The results showed the presence of the luteinizing hormone in discrete hypothalamic brain areas (Advis *et al.*, 1989).

Electrophoresis is a combination of two words; Electro meaning electric field and Phoresis meaning Migration. Due to the generated electric field and the resulting potential difference across the electrodes, positive molecules move to the cathode and negative molecules to the anode which is due to the potential generated between the electrodes.

This technique is of two types; Slap and Capillary electrophoresis. Electrophoresis is very sensitive but time consuming, bulky, and expensive (Reddy and Raju, 2012).

2.3.4 Mass spectrometry

This is an analytical technique that determines the molecular formula, weight, structure, protein sequence, and isotopic distribution in the sample under study. This technique has been demonstrated in understanding biological systems like enzymes, antibodies, hormones (Hale, 2013).

Mass spectrometry has been applied together with gas chromatography in the analysis of estrogen and testosterone hormones in isomers. Two different testosterone hormones; methyltestosterone (met-TEST) and nor- testosterone, (nor-TEST) were identified, and eight estrogen hormones; hexestrol (HEX), dien-estrol (DIEN), steroids 17- β -estradiol (βE_2), 17- α -estradiol (αE_2), 17- α -ethynlestradiol (αEE_2), and diethylstilbestrol (DES) were differentiated from estrogen (Garcia *et al.*, 2005).

Mass spectrometry coupled with Liquid chromatography has been applied to study meat, liver, and kidney tissues to determine hormonal chemicals that are naturally in existence and synthetic compounds like trenbolone, nandrolone among others. Hormonal chemicals were identified with the limit of detection ranging from 1 to 120 ng/kg (Shao *et al.*, 2005).

Four stages are involved during the process of mass spectrometry in the order of Ionisation, Acceleration, Deflection, and Detection (Aretz and Meierhofer, 2016). This detection technique is fast and small sample sizes are required though very expensive, do not give structural information directly, and require a lot of sample preparation.

2.4 Reproductive disorders associated with reproductive hormone level variation.

The reproductive system is important in the body in both males and females. The female reproductive system is under the threat of various reproductive disorders that include infertility, dysmenorrhea, breast cancer to mention but a few. One of the major causes of these disorders is the hormonal variation that may result from medication used to manage reproductive disorders.

2.4.1 Dysmenorrhea (menstrual cramps)

Dysmenorrhea is a gynecological disorder caused by prostaglandin production during menses. It is experienced by most women at the postpubescent stage (Kaaria *et al.*, 2019). Dysmenorrhea is categorized into two classes; primary and secondary dysmenorrhea. Secondary dysmenorrhea is an elevated health condition of primary dysmenorrhea that causes identifiable pelvic disease (Dawood, 1984). Primary dysmenorrhea (Menstrual pains) causes stomach irritation, ulcers, nausea, vomiting, and sometimes diarrhea which results from the increment in the release and synthesis of prostaglandins from uterine endometrium at the beginning or during menstruation in form myometrium contraction. Primary dysmenorrhea does not lead to the pelvic disease. The contractions cause labor like, colicky and spasmodic pains in the lower back and abdomen that may last for several days (Jaafarpour *et al.*, 2015).

A correct diagnosis for primary dysmenorrhea is always made after a detailed historical study of the patient. If primary dysmenorrhea is not managed early enough it results in secondary dysmenorrhea. Usually, secondary dysmenorrhea is suspected in any female with a history of menstrual pains for more than two years (Dawood, 1984).

Medications to treat reproductive disorders have been found to alter the functioning and performance of the reproductive system. The alteration is usually evident in the changes in the reproductive cycle which results in a condition known as hormonal variation (Westwood F.R, 2008).

In Wistar rats, the reproductive cycle has four phases; proestrus, estrus, metestrus, and diestrus. This cycle is usually four to five days. The estrus phase lasts twenty-five to twenty-seven hours and there is no bleeding, proestrus lasts twelve to fourteen hours and the rats are on the heat. If mating occurs; the rats conceive.

Rats undergo the metestrus phase that lasts six to eight hours when there has not been any conception and during the diestrus phase which lasts fifty-five to fifty-seven hours (Westwood F.R, 2008).

2.5 Female Reproductive Hormones

Sex hormones are very important for regulating biological body systems particularly the Central nervous system which makes hormonal imbalance detection a highly relevant study field (Lightfoot, 2008). Four hormones regulating ovulation are;

- Estradiol
- Progesterone
- Follicle Stimulating Hormone (FSH)
- Luteinizing hormone (LH)

Estradiol hormone is produced from adrenal glands and ovaries. Estradiol hormone is important in reproductive system development, especially during the menstrual cycle.

Progesterone hormone is released by ovaries and is essential in the development of the uterine walls for implantation to take place and pregnancy maintenance (Patil *et al.*, 2015). Follicle Stimulating hormone and luteinizing hormone are released by the anterior pituitary gland under the influence of gonadotrophin-releasing hormone. Both hormones are synergistically responsible for folliculogenesis, oogenesis, and ovulation.

The female reproductive hormones are of different molecular formulae and different bonds of vibration. Luteinizing hormone has a molecular formula of $C_{60}H_{23}N_{15}O_{13}$ with C-C, C-O, O-H, C-N, NH-H, N-NH, C-N, C=O, N-H, and C-NH bonds of vibration (Heitman *et al.*, 2009). Follicle Stimulating hormone has a molecular formula of $C_{79}H_{125}N_{19}O_{23}S$ with C=O, C=N, C=C, C-S, S-H, C-O, O-H, C-H, and C-NH bonds of vibration. Progesterone has a molecular formula of $C_{21}H_{30}O_2$ with CH_3 , C=O, C-H, and C-C bonds of vibration (Sitruk-Ware and El-Etr, 2013). Estradiol has a molecular formula of $C_{18}H_{24}O_2$ with CH_2 , CH_3 , C-OH, C-C, and C=C bonds of vibration (Zhang *et al.*, 2007).

Reproductive hormone variation is among the causes of infertility hence maintaining a normal hormonal range is vital. A balanced hormonal system leads to the proper functioning of the reproductive system (Naveed *et al.*, 2015).

Hormonal imbalance has been known to be the main cause of Polycystic Ovary Syndrome PCOS which is the formation of cysts in the ovary (Webb *et al.*, 2018). This leads to irregularities in the menstrual cycle, infertility, back pain, hair loss, breast cancer, miscarriage, heart failure, weight gain, and other skin conditions.

Wistar rats were administered herbal extract and ibuprofen in this study as a treatment for reproductive disorders and their influence on the female sex hormones is studied. Sex hormones control the physical and biological activity of the body.

Wistar rats have a short and regular oestrus cycle that is controlled by various female reproductive hormones. The short cycle has made rodents ideal for various studies and research. The oestrus cycle is made up of proestrus, estrus, metestrus, and diestrus stages (Caligioni, 2010).

- The proestrus stage is described by nucleated epithelial cells that occur as either individual or cluster form. It is the preovulatory day and the levels of estradiol increase as the levels of LH and FSH surge in the course of the night.
- The estrus stage is predominant of clustered cornified squamous epithelial cells. The levels of Estradiol are high in the morning and reduce in the afternoon. The levels of LH, FSH, and progesterone are low.
- The metestrus stage is characterized by leucocytes and either cornified squamous or/and nucleated epithelial cells. The levels of estradiol, LH, and FSH are low while the levels of progesterone remain high.
- The diestrus stage is characterized by leukocytes cells and the levels of estradiol hormone begin to increase.

2.6 Medication for Reproductive disorders

Various medications are administered to manage reproductive disorders including infertility, miscarriage, dysmenorrhea, among others. The medication can be natural herbs like *Asparagus racemosus* or conventional drugs like acetaminophen, ibuprofen, paracetamol obtained from the pharmacy.

Most developing countries depend on herbal medicine for diagnosis and around 80% of people use herbal medicine instead of chemical drugs for primary health care. Medicinal herbs have become an interesting area of research for the treatment of different diseases and health disorders.

2.6.1 *Asparagus racemosus*

Asparagus racemosus is a medicinal plant used to treat illnesses like ulcers, diabetes, nervous disorders, prevent aging, increase milk production in nursing mothers, improve immunity and mental function due to its antioxidant activity, manage dysmenorrhea and other female reproductive disorders (College, 2013). The plant is known for its great benefits in improving overall health especially of the female reproductive system (Sharma, 2011).

Asparagus racemosus is a climbing plant of the *Asparagaceae* family that grows one to two meters tall. It has thin needle-like leaves, bears white flowers with small spikes.

The roots of *Asparagus racemosus* are cluster-like fingers and tuberous and administered as medicine for the treatment of diseases affecting the female reproductive system (Shashi *et al.*, 2013).

The roots of *Asparagus racemosus* raise the levels of the female reproductive hormones (estrogen, progesterone, Luteinizing hormone LH and Follicle Stimulating hormone FSH) and the maximum increase was evident when the high dose (more than 500 mg) of the natural herb was administered (Sharma, 2011).

The roots of the herb are dried and grounded to form a powder which contains elements like vitamin B, Calcium, Zinc, amino acid compounds like arginine and aspartic acids that are essential in females' health and proper functioning of the female reproductive system making it vital in the diagnosis of menstrual disorders such as menstrual cramps, irregular bleeding, premenstrual syndrome, and management of hormonal balance during ovulation and menstruation cycle. Arginine and aspartic acid stimulate and regulate the release of FSH and LH (Kaaria *et al.*, 2019). This herbal formulation has been found very essential in the treatment of disorders associated with menstruation and menopause, enhancing ovulation hence improving fertility since it increases the chances of conception when the right dose is administered (Sharma, 2011).

In this research, blood and vaginal fluid samples obtained from Wistar rats to which this medicinal plant had been administered to detect hormonal variation with Raman Spectroscopy technique and study the influence of the herbal extract on the reproductive hormones.

2.6.2 Ibuprofen

Ibuprofen is a nonsteroidal anti-inflammatory drug (NSAID) that is used in the treatment of fever and effective in providing relief from pains caused by menstrual cramps (primary dysmenorrhea), toothache, back pain, and other body pains. During the action of this drug, the hormones that cause pain in the body are reduced (August *et al.*, 2017).

Ibuprofen has been administered to specifically manage menstrual cramps since it does not affect the metabolic behavior and pituitary ovarian axis making it a better medication to manage dysmenorrhea with very minor or no side effects (Dawood, 1984). This drug causes fluctuations in the uterine hypercontractility hence alleviating pain (Dawood and Khandawood, 2007).

During the administration of ibuprofen, the right dose should be administered. Overdose causes health complications to body organs like the heart, liver, kidney, and body systems like the reproductive system hence affecting fertility. The recommended and right dose of ibuprofen for rats is 20 mg/Kg, a low dose is 10 mg/Kg, and overdose 50 mg/Kg.

Raman Spectroscopic technique coupled with chemometric data analysis tools in the detection of hormonal variation in blood and vaginal fluid of the female Wistar rats has the potential to overcome the challenges being faced with the conventional detection methods (ELISA, HPLC, electrophoresis) that include being complex, label dependant, requiring tedious sample preparation procedures, not able to give instant results hence time-consuming. The fact that small samples are needed together with the rapidity of obtaining results makes Raman spectroscopy coupled with chemometric a better tool in the quick screening of a large population. The potentiality of Raman spectroscopy together with chemometric analysis tools is expected to revolutionize research on fertility studies in human beings since rats have a similar reproductive system to that of humans (Sengupta, 2013).

CHAPTER THREE: THEORETICAL FRAMEWORK

3.1 Chapter Overview

In this chapter, the theoretical framework of Raman Spectroscopy, data pre-processing, and the chemometric analysis tools focusing on PCA and ANN are discussed.

3.2 Raman spectroscopy

Raman Spectroscopy is a diagnostic technique that is used to study vibrational, rotational and any low-frequency modes of any given sample under study. Raman spectroscopy depends on the shining of laser light whereby photons incident to a sample lose or gain energy after interacting with excited molecules in a sample, scattered light with less energy (Stokes Raman) and that of more energy (Anti-Stokes Raman) is then measured (Agarwal and Atalla, 2008). It depends on either Raman or Inelastic scattering of monochromatic light in the near-infrared, ultraviolet or visible range in the electromagnetic spectrum. Raman Spectroscopy is commonly used in conjunction with Fourier transform Infrared (FT-IR) spectroscopic technique to obtain complete spectral data of the sample. Raman Spectroscopy obtains spectral profiles showing peaks and valleys displaying different sample rotational and vibrational transitions.

With the Raman Spectroscopic technique, the sample to be analyzed is illuminated with laser light and wavelengths of the scattered light almost equal to that of the laser light are filtered out and the unfiltered light is directed to the detector due to Rayleigh scattering.

With Raman spectroscopy, the laser light is like an electromagnetic wave. When the electric field E is introduced into a sample, it causes a disturbance in the molecular electron orbits, hence induction of a dipole moment p (Sato-berrú *et al.*, 2004). The induced dipole moment is directly proportional to the electric field (Hahn, 2007).

$$p = \alpha \bar{E} \quad (3.10)$$

α is the electric polarizability tensor which depends on the shape and the chemical bond dimensions.

The electric field E is given by;

$$E = E_0 \cos \omega t$$

$$\omega = 2\pi\nu_0$$

$$E = \bar{E}_0 \cos (2\pi\nu_0 t) \quad (3.11)$$

ν_0 is the vibrational frequency of the radiation.

The electric polarizability tensor α depends on the molecule with mode coordinates Q . Using the Taylor series this dependence relation can be expanded.

$$\alpha = \alpha_0 + \sum_k \left(\frac{\partial \alpha}{\partial Q_k} \right)_0 Q_k + \frac{1}{2} \sum_{k,l} \left(\frac{\partial^2 \alpha}{\partial Q_k \partial Q_l} \right)_0 Q_k Q_l + \dots \quad (3.12)$$

Q_k and Q_l are mode coordinates that correspond to the k^{th} and l^{th} vibrational modes corresponding with the vibrational frequencies ν_k and ν_l .

Considering the first two terms in the equation (3.12), the corresponding mode vibration equation reduces to;

$$\alpha_\nu = \alpha_0 + \alpha'_\nu Q_\nu \quad (3.13)$$

α'_ν represents polarizability tensor derivative to the mode vibration Q_ν at equilibrium.

The modes vibrate according to the harmonic oscillator, hence the mode function Q_ν varies with time as;

$$Q_\nu = Q_{\nu 0} \cos(2\pi \nu_\nu t + \varphi_\nu) \quad (3.14)$$

With $Q_{\nu 0}$ being the mode amplitude vibration, and φ_ν the phase angle.

When equation (3.14) is substituted into equation (3.13), it yields;

$$\alpha_\nu = \alpha_0 + \alpha'_\nu Q_{\nu 0} \cos(2\pi \nu_\nu t + \varphi_\nu) \quad (3.15)$$

This shows that the polarizability tensor experiences a harmonic oscillation of frequency (ν_ν) equal to the vibrational frequency of the molecule's mode coordinate.

By substituting equation (3.11) and equation (3.15) in equation (3.10), then the induced electric dipole moment is given as;

$$p = [\alpha_0 + \alpha'_\nu Q_{\nu 0} \cos(2\pi \nu_\nu t + \varphi_\nu)] \bar{E}_0 \cos(2\pi \nu_0 t) \quad (3.16)$$

Simplifying further, equation (3.16) becomes;

$$\begin{aligned} p &= \alpha_0 E_0 \cos(2\pi \nu_0 t) + \alpha'_\nu E_0 Q_{\nu 0} \cos(2\pi \nu_\nu t + \varphi_\nu) \cos(2\pi \nu_0 t) \\ p &= \alpha_0 E_0 \cos(2\pi \nu_0 t) + \frac{1}{2} \alpha'_\nu E_0 Q_{\nu 0} \cos[2\pi(\nu_0 + \nu_\nu) t + \varphi_\nu] + \\ &\quad \frac{1}{2} \alpha'_\nu E_0 Q_{\nu 0} \cos[2\pi(\nu_0 - \nu_\nu) t - \varphi_\nu] \end{aligned} \quad (3.17)$$

Therefore, the induced dipole moment is a function of two frequencies, that is the vibrational frequency of the molecules (ν_v) and the frequency of the incident radiation (ν_0), which is further simplified to;

$$p = p(\nu_0) + p(\nu_0 + \nu_v) + p(\nu_0 - \nu_v) \quad (3.18)$$

From the equation (3.18), the induced dipole moment consists of 3 components. Each component has a particular dependence on frequency.

The first term of equation (3.18) refers to elastic scattering of incident radiation whereby the frequency of the induced dipole moment is the same as that of the incident radiation hence the same energy. This is referred to as Rayleigh scattering. The third and second terms in the equation correspond to inelastic scattering whereby the induced dipole moment and the incident radiation have different frequencies. The second term represents scattered photons with more frequency and energy than that of the incident photons (Anti-stokes scattering), while the third term represents scattered radiation with energy less than that of the incident photons (Stokes scattering). The different types of scattering are shown in figure 3.1.

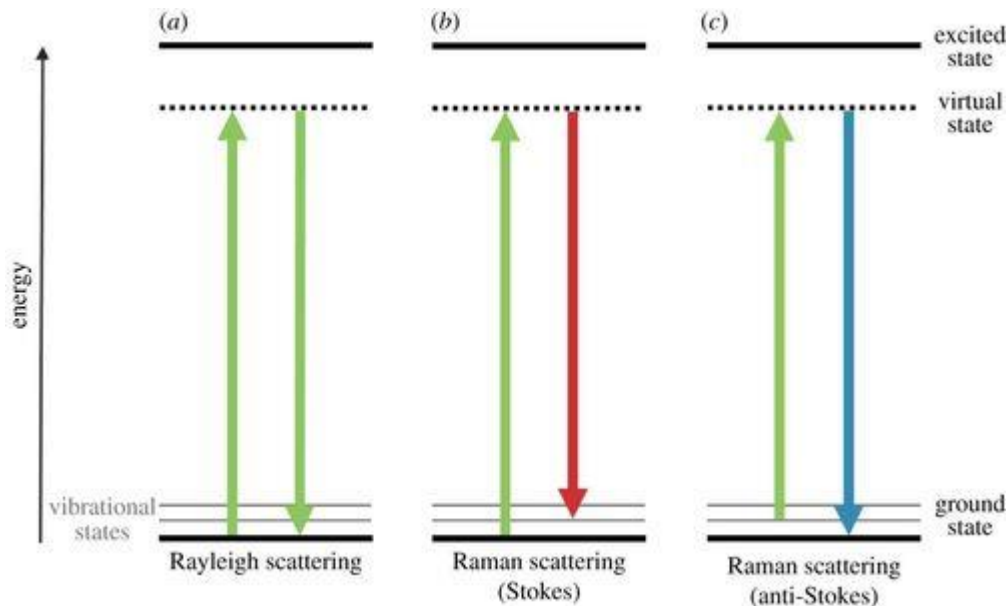


Figure 3. 1: Diagram of Raman and Rayleigh Scattering (Moura et al., 2016)

For incident EM radiation on the molecules, there is the absorption of energy and radiations move to the higher virtual level above the ground level, and the differences in quantum numbers between the initial and final state should be equal to 0 or ± 1 . If it equals 0, it is considered to be Rayleigh scattering, otherwise its anti-Stokes or Stokes Raman scattering.

According to Boltzmann distribution function, molecules occupy various vibrational energy levels at room temperature, but according to the Schrodinger equation describing a particle in a shell, there is a small number of energy levels permitted with the lowest level being heavily populated. Molecular bonds do confine the atoms to specific quantized vibrational modes where vibrational energy levels are given as;

$$E_v = (v + \frac{1}{2}) h\nu_v \quad (v = 0, 1, 2, \dots) \quad (3.19)$$

Where ν_v is the vibrational frequency, v is the vibrational quantum number of individual atoms, h is the Planck's constant.

Figure 3.2 below shows the vibrational and electronic energy states of a diatomic molecule.

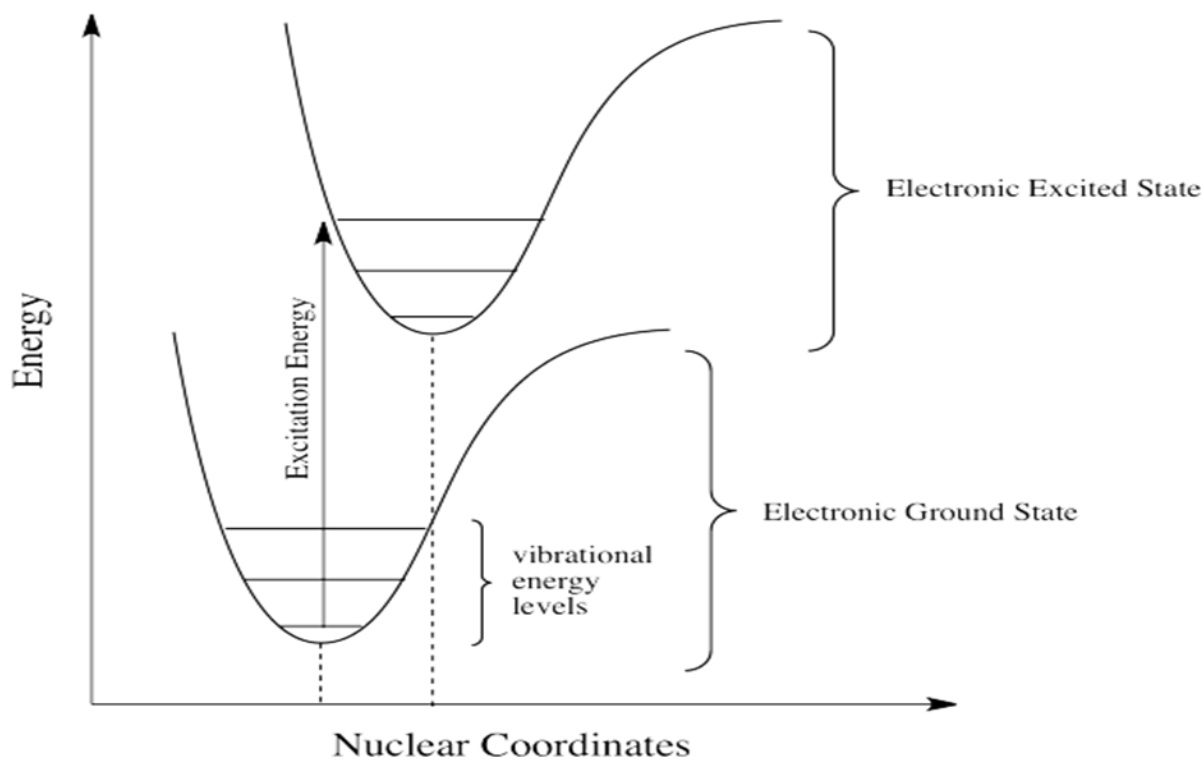


Figure 3. 2: A schematic diagram of the electronic and vibrational transitions for a diatomic molecule (Sato-berrú *et al.*, 2004).

With Raman spectroscopy, a laser (an intense light beam) shines on a sample, the dispersed radiation intensity is measured with its wavelength. The intensity and the Raman wavenumber $\bar{\nu}$ (cm^{-1}) are plotted. The wavenumber is given by:

$$\bar{\nu} = \frac{1}{\lambda(\text{incident})} - \frac{1}{\lambda(\text{scattered})} = \frac{\nu_m}{c} - \frac{\nu_0}{c} \quad (3.20)$$

ν_m and ν_0 are the frequencies of the respective radiations and c is the speed of light.

This knowledge makes it possible for Spectro physicists to perform peak assignments for the identification of elements in a sample based on the Raman peaks. The Raman band position is influenced by the force of molecular bonds. For instance, the hydrogen atom has a single bond (O-H, N-H, C-H) at the peaks that lie between $3650\text{-}2750\text{ cm}^{-1}$, this region absorbs energy. Double bonds (-C=C-, -C=O) appear between $2250\text{-}1500\text{ cm}^{-1}$, then the other groups that do have complex patterns with many molecules have their Raman bands below 1500cm^{-1} . This information is therefore important during the interpretation and vibrational assignment of Raman spectra.

3.2.1 Raman setup and optimization

The specific laser suitable for use in Raman spectroscopy has to be of high intensity and with frequency stability. In this study we were interested in the Raman scattering only, the back-reflected laser and the Rayleigh scattering are reflected away by the bandpass filter. A monochromator sorts the scattered photons by wavelength before they are detected by a CCD camera. All spectrometers disperse light in terms of their wavelength. Light with different wavelengths is separated in a function of either time or space. In the Raman spectroscopy, there are two sets of spectrometers; the one uses the principle of diffraction of light and the other uses Fourier transform as shown in figure 3.3.

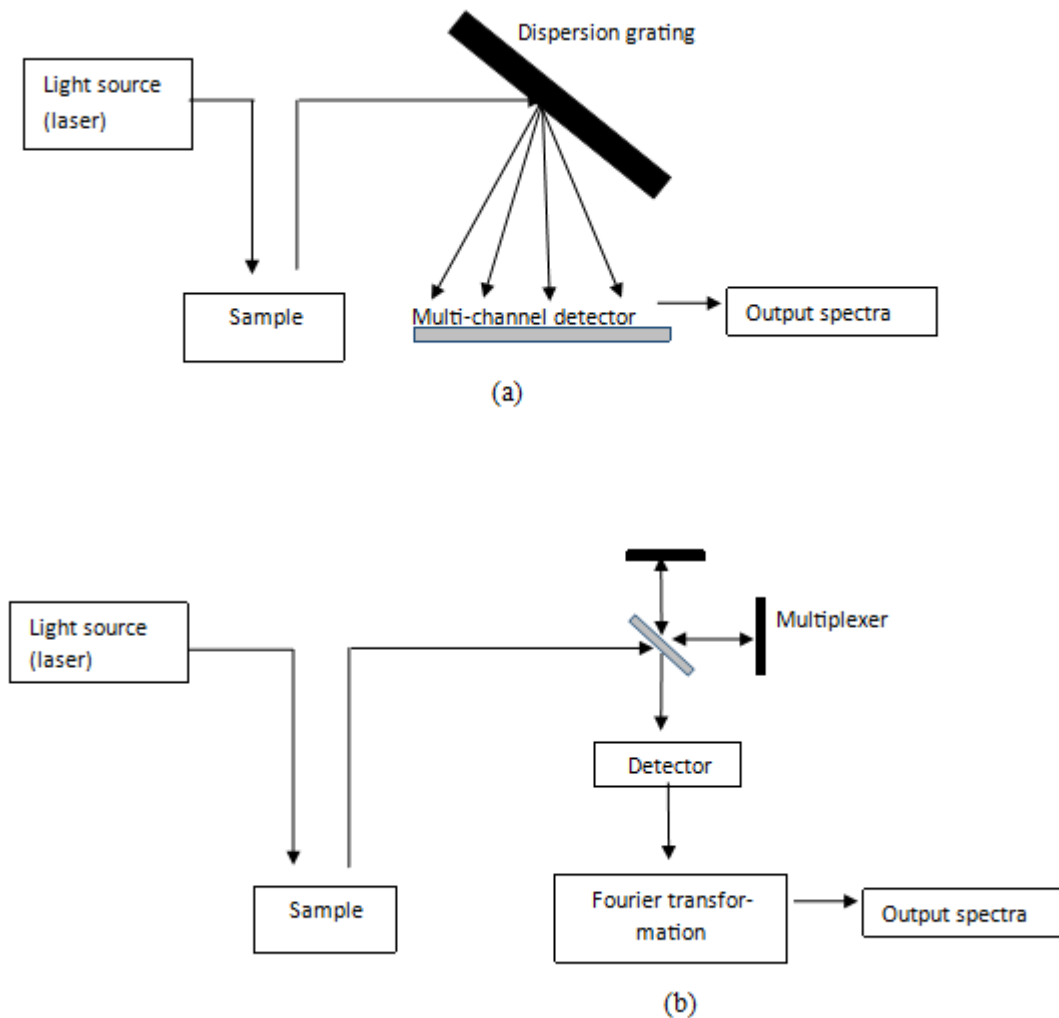


Figure 3. 3: (a) A general dispersive Raman spectrometer (b) Fourier transform (FT) Raman spectrometer (Dzsaber et al., 2015).

Optimization of the instrument is highly recommended by using proper standards and the correct choice of parameters to obtain optimum results. These include laser center wavelength, laser power, and laser beam size, exposure time of the laser-focused on the sample (ET), and the percentage of the laser intensity on the sample. These are to be considered carefully to obtain an optimal output spectrum.

3.2.2 Assignment of Raman Peaks

In Raman Spectroscopy, vibrations of different samples on the spectral curve take up different positions. The vibrations appear as peaks on the spectral curve which are assigned and interpreted concerning the type of bonds assigned for a particular spectral range. For each peak identified the type of bonds responsible is characterized by energy and frequency. The wavenumber for the identified peak confirms the correct vibrational assignment.

3.3 Spectral Data Pre-processing

Data pre-processing is a very fundamental process in any research that transforms collected data in preparation to main data analysis to remove variations and outliers in data that has no relationship to the analytical information (Shah *et al.*, 2007). Spectral data pre-processing involves various processes to be able to begin data analysis and these include the following;

Baseline correction is performed on the spectral data to have all the minimum values begin from zero and also correct distortion in the data (Ressom *et al.*, 2005).

Smoothing is done to eliminate the background noise in the obtained spectral data

Normalization is done to minimize the Raman intensity variation within the spectral data (Ressom *et al.*, 2005) and also avoid any unwanted effects resulting from different scales of the variables (Brereton, 2003).

$$X_{Normalised} = \frac{X_{actual} - X_{minimum}}{X_{maximum} - X_{minimum}} \quad (3.22)$$

Where;

$X_{normalised}$ is the normalized Raman intensity

X_{actual} is the Raman intensity for each spectrum

$X_{maximum}$ is the Raman intensity of the spectrum with the highest intensity values.

$X_{minimum}$ is the Raman intensity of the spectrum with the lowest intensity values.

Mean centering is performed to have all the input values scaled to have a standard deviation of one (1) and the mean of zero (0) (Varmuza and Filzmoser, 2016).

During data pre-processing the data set is reduced generating a new data set of variables that contain sums of the original weighted data achieved through applying mathematical techniques of linear combinations.

Data is manipulated to change the distribution of collected data variables to normal distribution. The values of the input variables are scaled to have a standard deviation of one (1) and mean value of zero (0) to be able to achieve equal statistical influence of the collected data hence generating a new data matrix to describe the relationship between variables. Data pre-processing is mainly done in data preparation before analysis to achieve the following (Park, 2000);

- i. To manipulate data into a suitable form for analysis.
- ii. To eliminate the variations in the data collected.
- iii. To obtain relevant information present in the data collected.

The processes performed on the data before analysis is performed to eliminate effects and noise caused by different ranges and scales.

3.4 Chemometric Analysis Tools

Chemometrics is defined as the science of applying mathematical and statistical tools to extract information and relate measurements obtained using Raman Spectroscopy. Usually, the data obtained (Raman spectra) is complex and multidimensional due to overlapping Raman bands making it necessary to apply statistical and mathematical methods to extract relevant information (Hanson, 2012). The spectra obtained are modified using chemometric tools to reduce its dimensions for quantification enabling the researcher to identify the differences, similarities, and correlations in the data collected.

3.4.1 Principal Component Analysis

Principal Component Analysis (PCA) is an unsupervised statistical and practical tool used in data analysis and is applicable in neuroscience, image compression, and face recognition that establishes the relationship in the experimental data to obtain hidden properties found in the data set obtained (Paul *et al.*, 2013). This data analysis technique is used to reduce the complexity of data to a lower dimension, find relationship patterns of similarities and differences in high-dimensional data (Ullah *et al.*, 2019). The dimensions of the data set are compressed through reduction without any loss of the information, main variables are selected, outliers are defined, and performs pattern recognition hence validation of the samples through clustering achieved through original data projection on the principal components. An original data matrix X of $(a \times b)$ dimension is reduced to;

$$X = MN^T \tag{3.23}$$

Where;

M is the $(a \times r_{max})$ the matrix representing the first principal component (PC1).

N^T is the transpose of N and is an $(b \times r_{max})$ representing the second principal component (PC2).

r_{max} is the number of components equivalent to the rank of X .

PCA uses the technique of eigenvalue analysis and the covariance matrix is used to extract data represented by a combination of eigenvectors of a training data set. PCA also reduces largely correlated variables to small uncorrelated variables known as Principal Components that are orthogonal to each other. The first principal component (PC1) is a linear latent variable that represents much variability in the data set. The second principal component (PC2) shows less minimal variance than PC1 of the scores, PC2 is orthogonal to PC1. The other principal components follow with reduced remaining variability.

3.4.2 Artificial Neural Networks

Artificial Neural Network is a supervised regression analysis technique that applies mathematical practical models suitable for building input and output-based models of multiple relationships through curve fitting to stimulating the functioning and structure of neural networks (Sensitivity and Trees, 2018). The networks are composed of interconnected neurons which are building blocks carrying information hence able for processing data that is fuzzy and incomplete. Inputs are fed into the mathematical model to obtain outputs. The working principle of ANN is guided by a mathematical model. A simple model is made of three functions that are summation, multiplication, and activation.

ANNs are applied to find solutions to problems that are quite challenging and solve them using classical algorithms. The working principle of ANN as a modeling tool to perform multivariate calibration has been well documented (Zhelavskaya *et al.*, 2018).

Each neuron can receive various inputs that are weighed and the sum biased against a threshold level that has been given. Neurons are interconnected and a signal can move from one neuron to another across different layers hence the signal is multiplied with a separate weight value.

The weighed inputs when summed up to form a nonlinear function is compared with the output to be able to come up with a range of fixed values. A problem is solved using the network when input values are applied to the output values in the first layer allowing the signal to move across the whole network and then give output values.

Some different neurons and parameters are very important in the network to form different layers that include; input, hidden layers, nodes, momentum, and iterations to give better optimization. The complexity of the ANN model depends on the number of hidden layers.

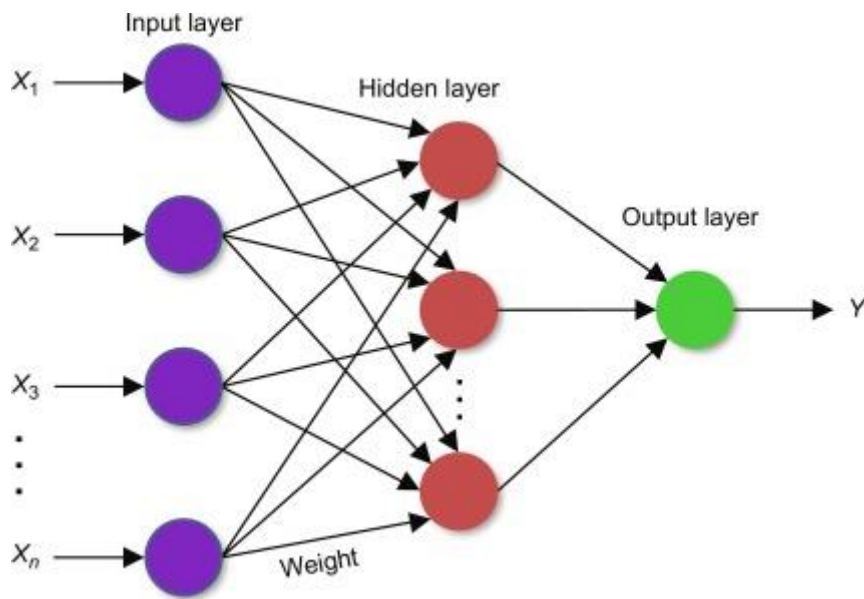


Figure 3. 4: Schematic flow of ANN (Sensitivity and Trees, 2018)

When networks are generalized, the simulation is performed on the input of the first layer. The signals can move across the different layers that are linked to each other by a certain weighting value.

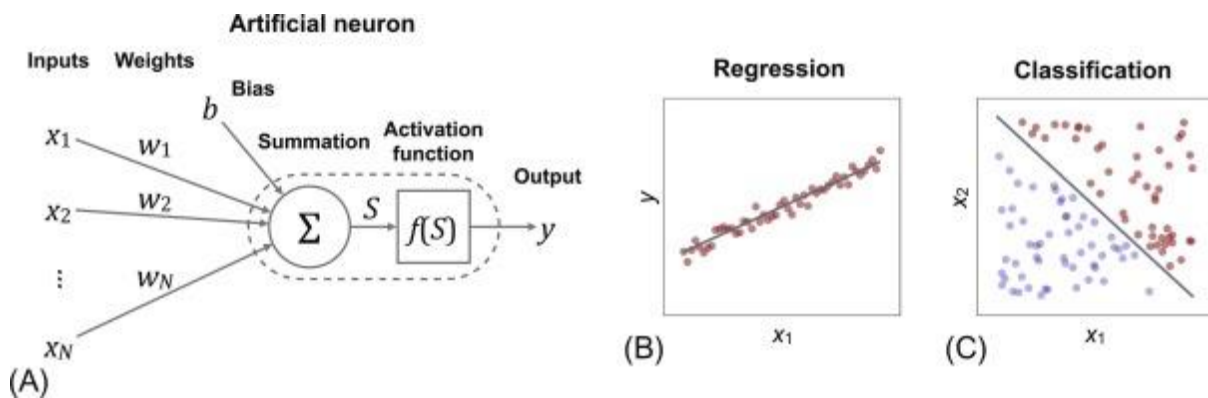


Figure 3. 5: (A) Diagram of an artificial neuron (B) Regression plot of obtained data and (C) Classification of the data collected on the sample (Zhelavskaya et al., 2018).

ANNs when well utilized can build multivariate calibration models that of the form;

$$Y = F(X) + \varepsilon \tag{3.24}$$

Where;

Y is a vector matrix of sample responses.

F is the network function

X is the matrix of measurements that have been carried out on various samples.

ε is the model prediction error.

Artificial Neural Networks are often referred to as artificial intelligence because of their ability to solve both regression and classification problems that cannot be solved with the traditional computational methods.

CHAPTER FOUR: MATERIALS AND METHODS

4.1 Chapter overview

This chapter discusses the different materials and methods that were used in this research. Raman spectroscopy was applied as a detection technique for hormonal variation in the female reproductive hormones for their vibrational and rotational bands when *Asparagus racemosus* (herbal extract) and ibuprofen were administered.

4.2 Materials

Different materials were used to successfully carry out this study. The conductive silver paste paint, NO VOC (SPI#04961-AB, 1 Troy Oz.(24ml), LOT#1221121) with a brush applicator cap manufactured by SPI Supplies Division of STRUCTURE PROBE, Inc in the USA is available at the Department of Physics, University of Nairobi and has been shown in figure 4.1 below.



Figure 4. 1: Conductive Silver paste/paint

Microscope glass slides ground edged made of clear glass of 25.4mmx76.2mm in dimension with a thickness of 1mm-1.2mm were obtained from the Department of Physics, University of Nairobi.

Wistar rats that were 5 to 6 weeks old from which blood and vaginal fluid samples were drawn were purchased and kept at the Department of Veterinary Anatomy and Physiology, University of Nairobi. 20 females and 1 male Wistar rats were purchased having a bodyweight of 180-200 g.

They were kept for two weeks to adapt to the environment in an animal nurturing room that was maintained at a temperature of 20-25 °C and a 12-hour day/night cycle. The rats were kept in the cages as shown in figure 4.2 below.



Figure 4. 2: Female Wistar rats stored in a cage

After two weeks, the female Wistar rats were divided into four groups of five animals in each group labeled HD for high dose, LD for low dose, IBU for Ibuprofen, and NRM for control or nontreated. These rats had access to water and food.

The *Asparagus racemosus* (herbal extract) roots were obtained from Nakuru, Kenya.

Ibuprofen (BRUFEN 400) manufactured by Abbott Laboratories (Pakistan) Limited was purchased from a pharmacy in Nairobi city.

Raman Spectroscopy is available at the Department of Physics, the University of Nairobi which was used to study the sample and obtain spectral profiles.

4.3 Methods

4.3.1 Preparation of the Raman substrate

Microscope glass slides were obtained, cleaned with ethanol, and allowed to dry for 10-20 minutes.

Conductive silver paste smears were then made on the cleaned microscope glass slides. Five patches of the silver paste were made on the microscope glass slides with a brush then left to dry for about 30-60 minutes. The spreading of the conductive silver paste is being demonstrated in figure 4.3 below.

Conductive silver paste is made of silver solids that are $40\% \pm 2\%$ per weight and an organic suspending and binder (10-30% n-Butyl acetate, 5-10% acrylic resin, and 10-30% 1-methoxy-2 propanol acetate) (Birech *et al.*, 2020).



Figure 4. 3: Spreading of the conductive silver paste on the microscope glass slide

The conductive silver paste was the substrate used for the enhancement of the Raman signal a process known as Surface Enhanced Raman Spectroscopy (SERS). The conductive silver paste was used because it is chemically stable, easy to prepare, and is relatively affordable compared to other substrates (Birech *et al.*, 2020) used for Raman signal enhancement like copper and gold.

4.3.2 Sample preparation

The *Asparagus racemosus* (herbal extract) roots were washed thoroughly well, dried, and grounded to obtain a powder form. The roots of *Asparagus racemosus* (herbal extract) that have been washed are shown in figure 4.4.



Figure 4. 4: Roots of *Asparagus racemosus* (herbal extract) after being washed.

When the roots in figure 4.4 above dried, they were grounded into powder shown in figure 4.5 below. The powder was then mixed with distilled water to form a solution given to the rats.



Figure 4. 5: Powder form of Asparagus racemosus roots

For low dose, 300 mg/kg weight of powdered *Asparagus racemosus* (herbal extract) was dissolved in 1 ml of distilled water then administered daily to the group labeled LD for fourteen (14) days using a pipette.

For a high dose, 600 mg/kg weight of powdered *Asparagus racemosus* (herbal extract) was dissolved in 1 ml of distilled water then administered daily to the group labeled HD for fourteen (14) days using a pipette.

Ibuprofen tablets displayed in figure 4.6 were pounded into powder form and the powder mixed with distilled water to make a solution.



Figure 4. 6: Ibuprofen tablets (Pharmacy in Nairobi Business Centre)

20 mg/kg weight of ibuprofen powder was dissolved in 1 ml of distilled water and administered daily to the group labeled IBU for fourteen (14) days using a pipette.

Normal saline was administered to the group labeled NRM daily for fourteen (14) days and this was the control or nontreated group using a pipette.

Blood samples were drawn from the tail tip of the Wistar rats which was first cleaned with ethanol, a simple cut on the tail was made and then gently squeezed to deposit the blood on the conductive silver smeared microscope glass slides as shown in figure 4.7 below. The vaginal fluid was obtained using a micropipette from the vagina of the Wistar rats on to the conductive silver smeared microscope glass slides. Five samples were prepared for each treatment daily and twenty (20) Raman spectra were obtained for each prepared microscope glass slide to which blood and vaginal fluid samples were deposited.

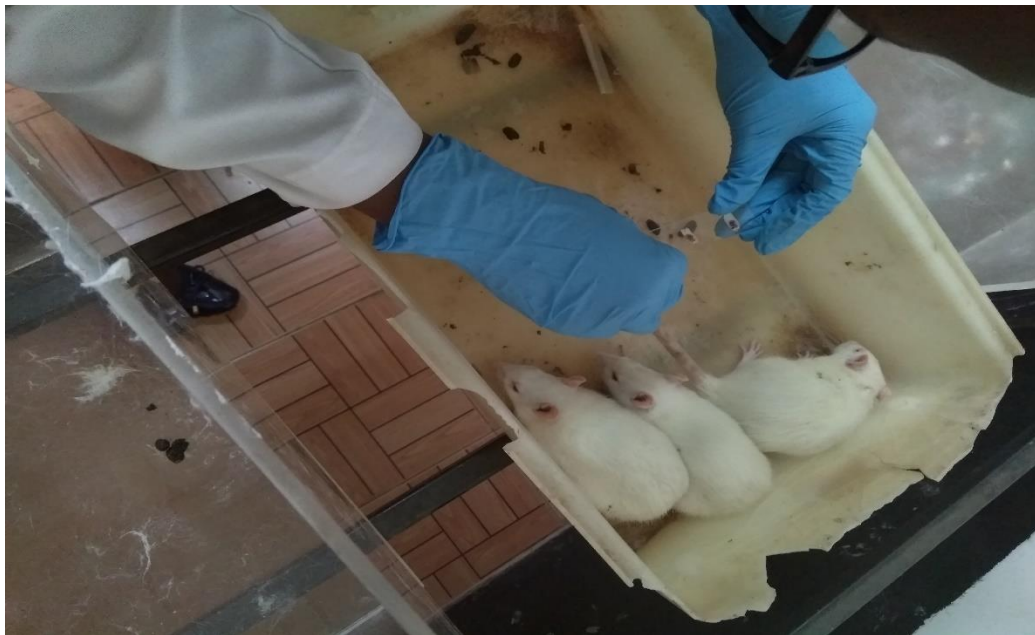


Figure 4. 7: Blood samples being deposited on the microscope glass slide.

Microscope glass slides to which blood has been deposited for all the group animals have been displayed in figure 4.8.

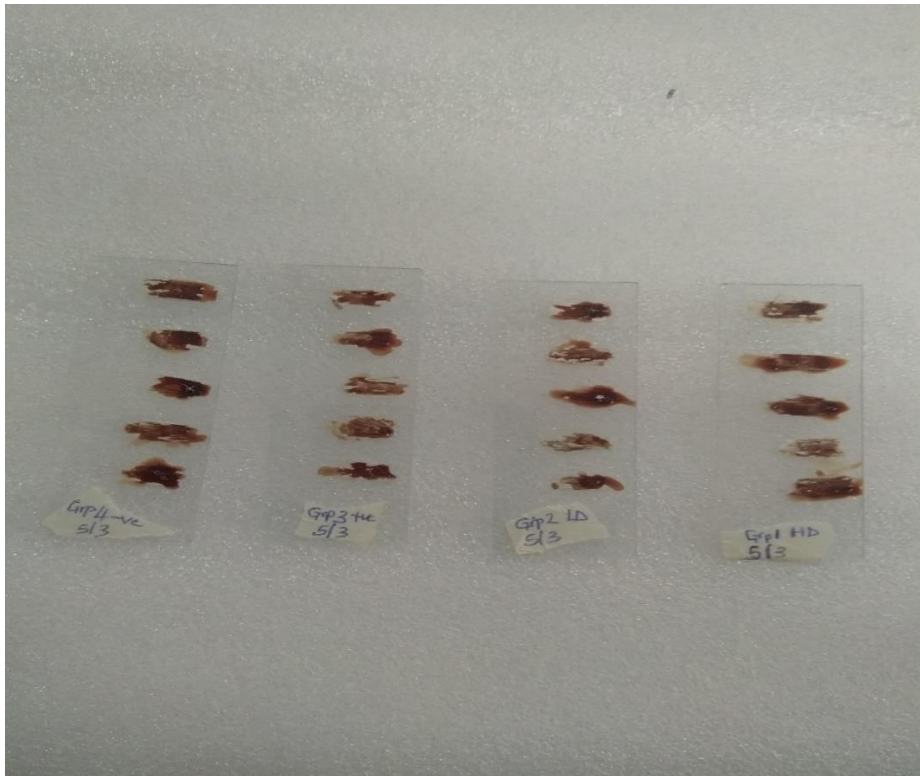


Figure 4. 8: Prepared blood samples ready to be studied with Raman Spectroscopy

Standard solutions of female reproductive hormones (Follicle Stimulating Hormone, Luteinizing hormone, Estradiol, and Progesterone) were obtained from the Anatomy and Physiology Department, University of Nairobi. Different concentrations of the standard solutions of the female reproductive hormones; 5 mlu/ml of Follicle Stimulating hormone, 5 mlu/ml of Luteinizing hormone, 0.2 ng/ml of Progesterone hormone, and 20 pg/ml of Estradiol hormone were deposited on conductive silver smeared microscope slides. Four samples were prepared for each hormone and twelve (12) Raman spectra obtained from each prepared sample.

The standard solutions of the female reproductive hormones were mixed with blood obtained from a male Wistar rat to obtain different concentrations of blood and the standard hormonal solutions have been tabulated in Table 4.1 below.

Table 4. 1: Different concentrations of male Wistar rat's blood mixed with standard solutions of female reproductive hormones (Follicle Stimulating hormone FSH, Luteinizing hormone LH, Estradiol, and Progesterone).

Female reproductive hormones	Concentrations
FSH (mlu/ml)	0.5, 0.83, 1, 1.25, 1.67, 2, 2.5, 3.3, 3.37, 4, 4.2, 5, 6.25, 6.7, 7.7, 8.0, 8.33, 10, 12.5, 16, 16.7, 18.7, 20, 21, 25, 33.3, 40 and 50.
Estradiol (pg/ml)	15, 16, 20, 24, 30, 40, 50, 60, 75, 80, 90, 96, 100, 120, 150, 200, 225, 240, 250, 300, 333.3 and 400.
LH (mlu/ml)	0.5, 0.83, 1, 1.25, 1.67, 2, 2.5, 3.3, 3.37, 4, 4.2, 5, 6.25, 6.7, 7.7, 8.0, 8.33, 10, 12.5, 16, 16.7, 18.7, 20, 21, 25, 33.3, 40 and 50.
Progesterone (ng/ml)	0.1, 0.2, 0.25, 0.33, 0.5, 0.67, 0.75, 2, 2.67, 4, 5.3, 6, 6.7, 8, 10, 13.3, 20 and 26.6.

For each prepared concentration of the standard solutions of the female reproductive hormone with male Wistar rat's blood, three samples were prepared and five Raman spectra were obtained. Twenty-eight (28) different concentrations were prepared for FSH and LH, twenty-two (22) for estradiol, and eighteen (18) for progesterone hormone.

This was done to be able to quantify data obtained from blood samples, determine the Limit of detection for Raman spectroscopy of each hormone and predict the concentrations of female reproductive hormones (Luteinizing hormone, Follicle Stimulating Hormone, Progesterone, and Estradiol) in the blood samples from the female Wistar rat. Male Wistar rat's blood was used because the female reproductive hormones in males are steady and nonfluctuating (Barp *et al.*, 2002).

4.3.3 Raman Spectroscopy Instrumentation

Raman spectroscopy technique was applied for hormonal variation detection in this study. Raman spectroscopy is a highly sensitive and molecular basic technique very handy for detection. Raman spectroscopy is always used in conjunction with Fourier transform Infrared (FT-IR) spectroscopic technique to obtain complete molecular information about the sample. Raman spectroscopy obtains spectral profiles of the samples being analyzed.

The Raman spectrometer (STR Raman Spectrum, Seki Technitron' Corp, Japan) at the Physics department, University of Nairobi can be fed with either 532nm or 785nm monochromatic lasers and a setup showing different parts of the Raman spectroscopy available at the Department of Physics, University of Nairobi is shown in figure 4.9 below.

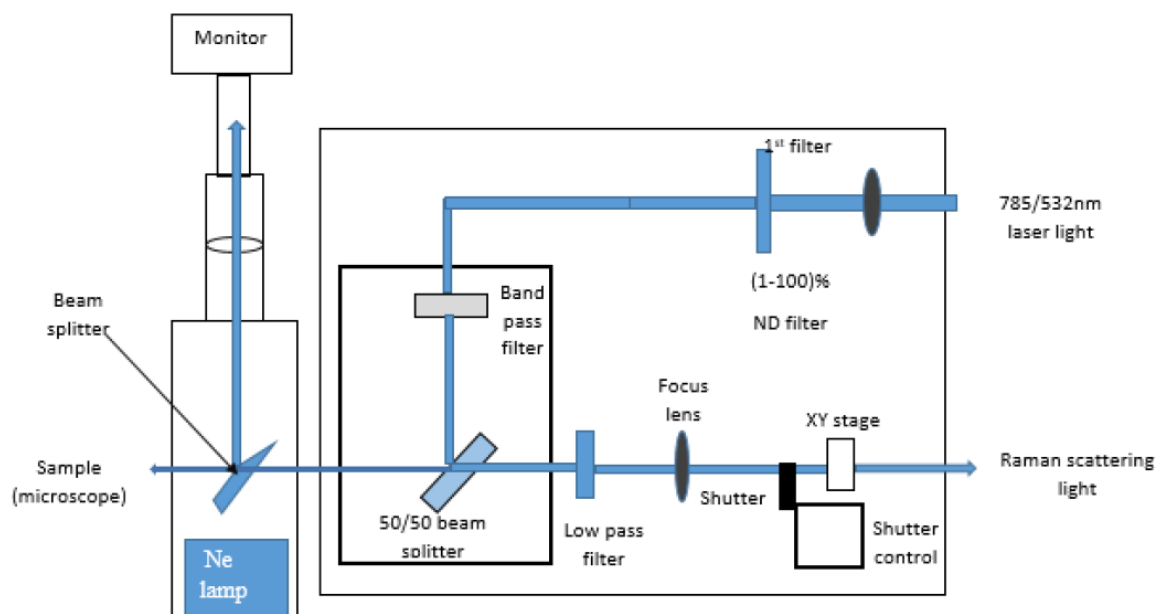


Figure 4. 9: Basic Raman set-up of Raman schematic (Terchnotron Corp Raman Spectroscopy manual 2012)

A laser beam of red or green light is directed to Raman Spectroscopy via an optical fiber allowing the beam to undergo total internal reflection. The beam is delivered to the bandpass filter according to the laser being used via the shutter. The light beam is then directed to the beam splitter that divides it into two equal portions; 50% is reflected and the other 50% is directed back to the sample to allow scattering that is measured by the imaging spectrometer and CCD camera.

The Spectrometer works with a grating of 1800, 1200, and 600 lines/mm grating and is fitted with a rear-scattered illuminated CCD camera to obtain spectral profiles of samples being examined.

Taking measurements is done in the darkroom to reduce fluorescence generated by the background light. Sample focusing is achieved using a motorized stage, computer with STR software, a microscope for visualization of various objective lens x10, x20, x50, and x100. Motor-driven stage assists in scanning through the sample at different spots to collect spectral data.

The spectrometer is always calibrated using a standard silicon wafer before any measurement is taken and a spectrum with a peak value of 519.56 cm^{-1} was obtained before analyzing the samples as displayed in Figure 4.10 below.

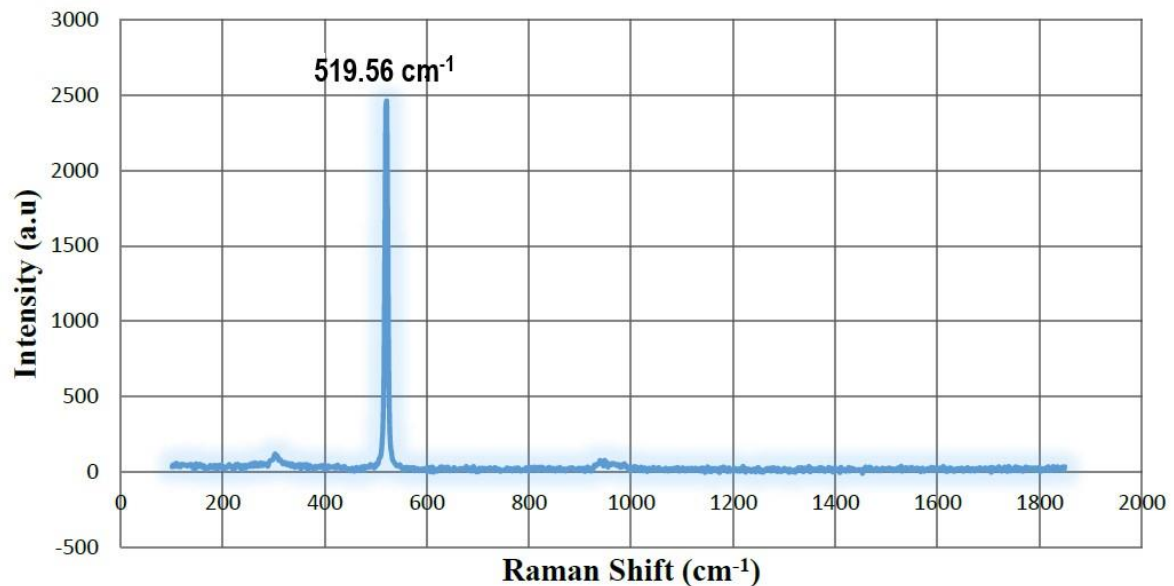


Figure 4.10: Raman spectrum for the standard silicon wafer using 785 nm laser.

4.3.4 Optimization of Raman Spectrometric Measurements

The optimization of measurements obtained using Raman spectroscopy is based on the region with the most vibrational bands of the sample under study. In this study, a 785nm laser was fed into the Raman spectrometer to collect the spectral profiles for each sample being prepared. The 785nm laser has been used because it produces less fluorescence in the spectrum as compared to the 532nm laser.

Specifications of x10 magnification objective lens, 0.3 Numerical aperture, 26.5 f-numbers, a grating of 600BLZ-750nm, the center wavelength of 1000 cm^{-1} , exposure time of 10 seconds, the number of accumulations was 5, spot size $68.47 \mu\text{m}$, and the power of 18.55mW was set before taking any measurement. The spectrograph was set at 256 X 1024-pixel CCD camera and the laser power was measured using the Orion Laser Power meter at different transmission intensities after and before the filter.

Table 4. 2: Laser power values at the different objective lens

Objective	Numerical Aperture	Power to sample		Laser Spot size	
		785nm (mW)	532nm (mW)	785nm (μm)	532nm (μm)
X10	0.3	18.2	6	68.47	10.02
X20	0.45	17.02	5.33	33.34	5.76
X50	0.5	8.52	5.6	14.6	1.56
X50	0.8	11.74	5.02	12.76	1.77
X100	0.9	6.34	4.7	6.02	0.625

The wavelength, numerical aperture, and laser spot diameter are related by the equation below (Quabis *et al.*, 2000)

$$LSD = \frac{1.22\lambda}{NA} \quad (4.1)$$

Where λ is the wavelength, LSD is the laser spot diameter and NA is the numerical aperture. Equation (4.1) implies that the 785nm laser has a lower spatial resolution than the 532nm laser.

Factors considered for optimization include; acquiring five Raman spectra from each spot on the microscope glass slide at different positions for an exposure time of 10 seconds for each spectrum after 5 accumulations. The spectra obtained for each spot were averaged to obtain a single spectrum.

The number of accumulations set for each spectrum to be obtained is another factor usually considered during the optimization of Raman spectrometric measurements. To come up with what number of accumulations to be considered, several tests have to be done to obtain the number of accumulations that give a high signal to noise ratio using the equation below (Quabis *et al.*, 2000).

$$SNR = \frac{I_p}{I_n} \quad (4.2)$$

SNR is signal to noise ratio, I_p is the intensity of the main band and I_n is the average intensity of the adjacent small peaks

4.4 Chemometric analysis of Raman spectra

The spectral data set obtained using Raman Spectroscopy is usually affected by so much fluorescence and background noise that have to be eliminated before the data analyzed. The data needs to be smoothed and baseline corrected.

4.4.1 Spectral data pre-processing

During data pre-processing, several actions were performed to be able to obtain a new spectral data set. Vancouver software was used to differentiate the Raman signal from the fluorescence signal which was set for the region ranging from 350 cm^{-1} to 1850 cm^{-1} . The Raman signal data was organized in Microsoft excel. Figure 4.11 shows two different spectra; before and after performing Vancouver on the Raman spectra obtained using Raman spectroscopy.

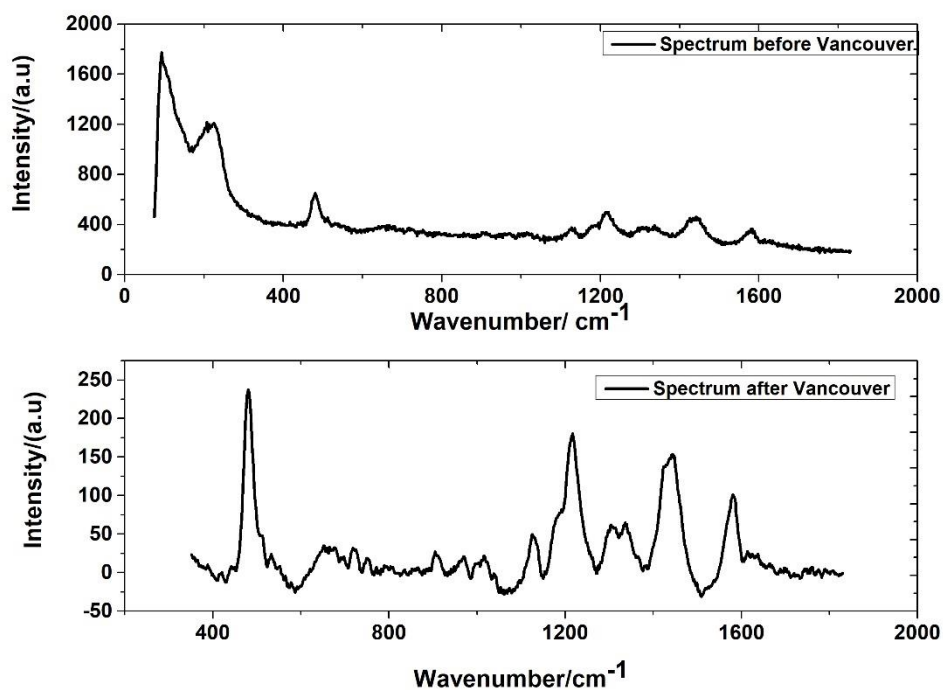


Figure 4. 11: Raman spectrum before and after the use of Vancouver software.

Baseline correction and normalization were performed in R software to have spectral data below zero eliminated. The baseline collected spectral data was then smoothed in Origin software to remove all the background noise. The spectral data were then normalized in R software in which the maximum intensity was subtracted from the actual intensity and then divided by the minimum intensity subtracted from the maximum intensity. PCA and ANN were then employed to the spectral data.

To identify significant differences in the obtained spectral data for both blood and vaginal fluid samples, we applied Analysis Of Variance (ANOVA) a statistical test in Microsoft Excel to obtain descriptive statistics in the data.

To define the patterns of similarity and differences, Principal Component Analysis was used and this was achieved through clustering and identification of Raman biomarker bands for each of the female reproductive hormones. Principal Component Analysis (PCA) on this spectral data was performed in R software. The script used to do PCA is documented in Appendix 1.

With Artificial Neural Networks, a mathematical model of three layers for each hormone was developed using the standard solutions of female reproductive hormones (Follicle Stimulating Hormone, Luteinizing hormone, Estradiol, Progesterone) mixed with blood obtained from a male Wistar rat as calibration standards regarding the spectral region around the Raman biomarker bands as the inputs. The ANN models were developed and built using R software and a script has been documented in Appendix 2.

The calibration data was composed of 15 simulate samples for each of the twenty-eight (28) different concentrations for LH and FSH, twenty-two (22) for estradiol, and eighteen (18) for progesterone hormones test data. A network of each model was developed using the Raman biomarker bands spectral region for each female reproductive hormone. A matrix of 15 by 28 for LH and FSH, 15 by 22 matrix for estradiol, and 15 by 18 matrix for progesterone hormone were used in the development of the ANN model for each hormone.

The spectral data set was saved as a CSV file and then imported to R software, it was then partitioned into different percentages of 70% to be the training data set and 30% to be the test data set. The model being developed was validated using k fold cross-validation, trained using the resilient backpropagation algorithm with three neurons in the hidden layer.

The performance of the model being developed was assessed by determining these values; Root Mean Square Error (RMSE), determination coefficient (R^2) and Mean Absolute Error (MAE) which are mathematically defined by the following equations;

$$MAE = \sqrt{\frac{\sum_{i=1}^n |A_i - P_i|}{n}} \quad (4.3)$$

$$RMSE = \sqrt{\frac{\sum_{i=1}^n (A_i - P_i)^2}{n}} \quad (4.4)$$

$$R^2 = 1 - \frac{\sum_{i=1}^n (A_i - P_i)^2}{\sum_{i=1}^n (A_i - \bar{A}_i)^2} \quad (4.5)$$

$$S.D = \sqrt{\frac{\sum_{i=1}^n (A_i - \bar{A}_i)^2}{(n-1)}} \quad (4.6)$$

Where A_i is the actual concentration value.

\bar{A}_i is the average actual concentration value.

P_i is the predicted concentration value.

n is the total number of samples.

CHAPTER 5: RESULTS AND DISCUSSION

5.1 Characteristic Raman spectra of standard female reproductive hormones

Solutions of female reproductive hormones of Follicle Stimulating Hormone (5 mlu/ml concentration), Luteinizing hormone (5 mlu/ml concentration), Estradiol hormone (20 pg/ml concentration), and Progesterone hormone (0.2 ng/ml concentration) were separately applied onto the conductive silver paste smeared microscope glass slides and Raman spectra measured after exciting with a 785 nm laser. This gave the characteristic Raman spectra of each of the respective hormones. Figure 5.1 shows the average Raman spectra (of 12 spectra each) obtained from the respective hormones (Follicle Stimulating Hormone, Luteinizing hormone, Estradiol, and Progesterone).

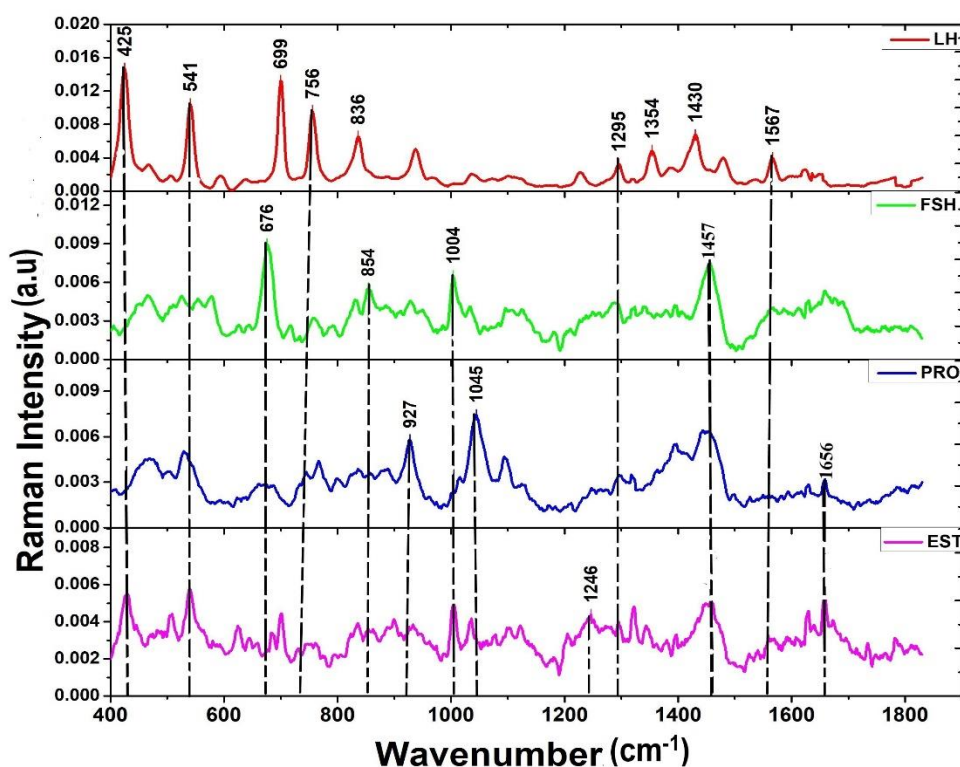


Figure 5. 1: Average characteristic Raman spectra of the female reproductive hormones standards Follicle Stimulating hormone, Luteinizing hormone, Estradiol and Progesterone with unique bands centered at 679, 1354, 1246, and 927 cm^{-1} respectively.

It was found that the Raman spectra of all the four hormones shared a common band centered at wavenumber 1295 cm^{-1} , Luteinizing hormone, progesterone, and Estradiol shared a common band centered at 541 cm^{-1} , Follicle Stimulating hormone, progesterone, and Estradiol shared a band centered 1457 cm^{-1} . Estradiol shared common bands with Luteinizing hormone, Follicle-stimulating hormone, and progesterone centered at wavenumbers 425 , 1004 , and 1656 cm^{-1} respectively. Progesterone shared common bands with Luteinizing hormone and Estradiol centered at 756 and 1656 cm^{-1} respectively. Luteinizing hormone and Progesterone shared a common band centered at 1567 cm^{-1} .

Unique bands were centered at 699 , 1354 , and 1430 cm^{-1} for Luteinizing hormone, 679 , and 854 cm^{-1} for Follicle Stimulating Hormone, 927 , and 1045 cm^{-1} for Progesterone, and 1246 cm^{-1} for Estradiol.

The bands can be associated with some components including amide I proteins (1656 cm^{-1}) (Jenkins *et al.*, 2005, Herrero, 2008) in Progesterone and Estradiol, amide III proteins (1295 cm^{-1}) (Herrero, 2008) in all the four hormones. The bands associated with tryptophan were centered at around 756 , 541 cm^{-1} (Ullah *et al.*, 2019), and 1567 cm^{-1} (Herrero, 2008) seen in Luteinizing hormone and progesterone respectively. The bands ascribable to Tyrosine were centered at 836 cm^{-1} in Luteinizing hormone and 679 cm^{-1} in Follicle-stimulating hormone (Herrero, 2008).

For vibrational assignments, the band centered at 756 cm^{-1} was tentatively assigned to C-H out of plane vibration (Bright *et al.*, 2010), 1656 cm^{-1} to C=C stretching vibration (Vedad *et al.*, 2018), 1295 cm^{-1} to CH_2 stretching (Minaeva *et al.*, 2008, Bright *et al.*, 2010) and 699 cm^{-1} to CH_2 twisting vibration (Bright *et al.*, 2010).

5.2 Principal Component Analysis for Raman spectra of standard female reproductive hormones

Principal Component Analysis (PCA) on the combined spectral data set of the standard hormones (LH, FSH, Estradiol, and Progesterone) was done to identify subtle spectral patterns that differentiate between spectra from each of them. This analysis was performed in R software. Figure 5.2 shows the 3D PCA score plot showing distinct segregation of the spectral data sets from each of the hormones.

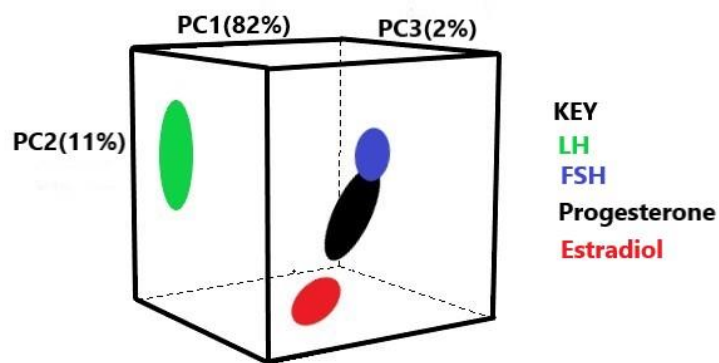


Figure 5. 2: PCA 3D score plot of Raman spectral data set of the female reproductive standard hormones.

In figure 5.2, the first, second, and third principal components explained 82% of the overall variation, 11%, and 2 % respectively. The distinguished four clusters consisted of estradiol, Follicle Stimulating Hormone, Luteinizing hormone, and progesterone implying that each hormone is different from other hormones. The different clusters shown in figure 5.2 were due to different concentrations of the hormones and the different components present in each hormone.

The loadings plot of the hormones shown in figure 5.3 was used to identify the peaks for each hormone responsible for the segregation.

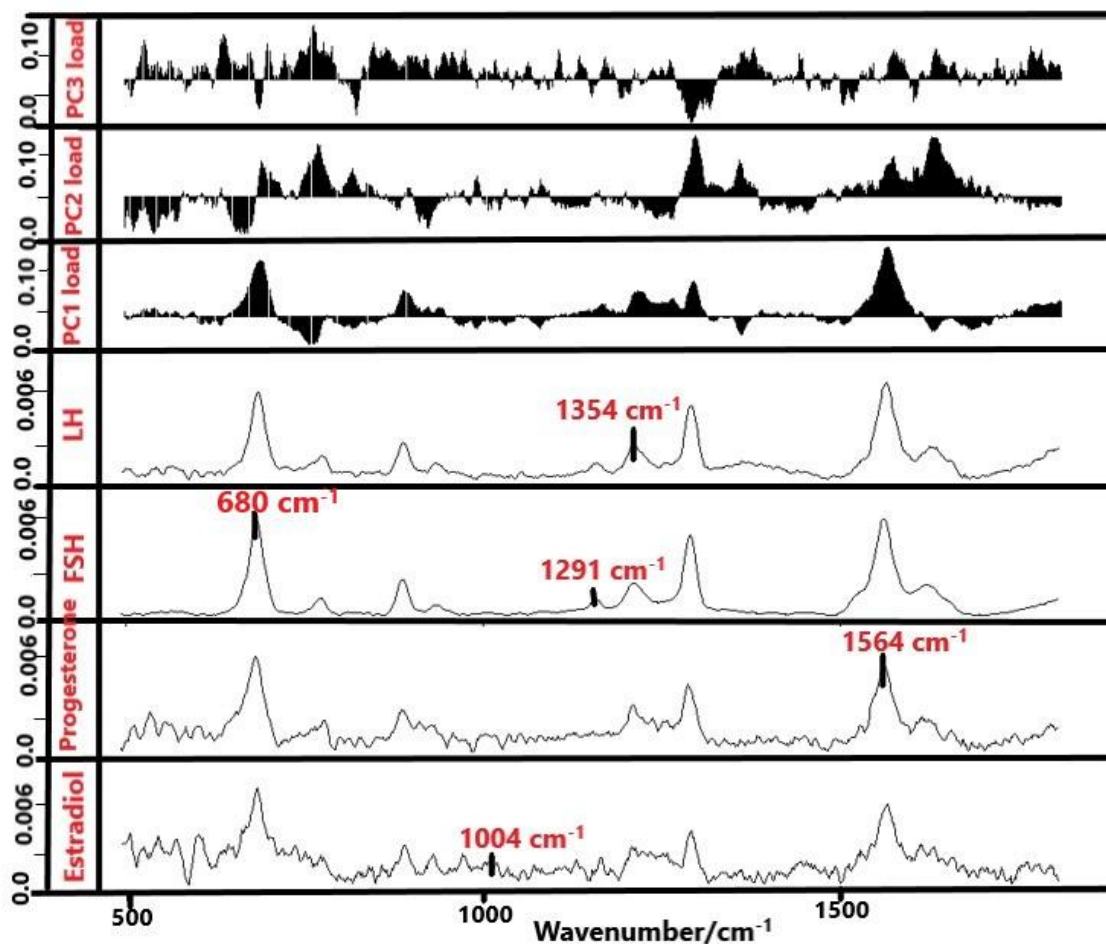


Figure 5. 3: Loading plots together with Raman spectra of Luteinizing hormone, Follicle Stimulating Hormone, Progesterone, and Estradiol hormones.

The loadings plot displayed in figure 5.3 shows that the bands responsible for the spectral segregation were 1354 cm^{-1} in Luteinizing hormone, 680 and 1291 cm^{-1} in Follicle Stimulating Hormone, 1004 cm^{-1} in Estradiol, and 1564 cm^{-1} in Progesterone spectra. This shows that the spectra from each of the hormones had unique profiles and supporting results displayed in figure 5.1.

5.3 Raman Spectra of standard female reproductive hormones mixed with Wistar rat's blood.

To facilitate identification of Raman biomarker bands and eventual application of Raman spectroscopic technique in the detection of the female reproductive hormones (Follicle Stimulating Hormone (FSH), Luteinizing hormone (LH), Estradiol and Progesterone), the solutions of these female reproductive hormones mixed with male Wistar rat's blood were investigated.

Different concentrations of Follicle Stimulating hormone (0.5, 3.3, 8.0 and 20 mlu/ml), Luteinizing hormone (0.83, 2.5, 6.25 and 16 mlu/ml), Progesterone (0.1, 0.67, 2 and 8 ng/ml) and Estradiol hormone (15, 90, 200 and 240 pg/ml) were selected randomly from the different concentrations that were prepared.

Figure 5.4 shows the average Raman spectra of selected concentrations of each of the female reproductive hormones mixed with male Wistar rat's blood.

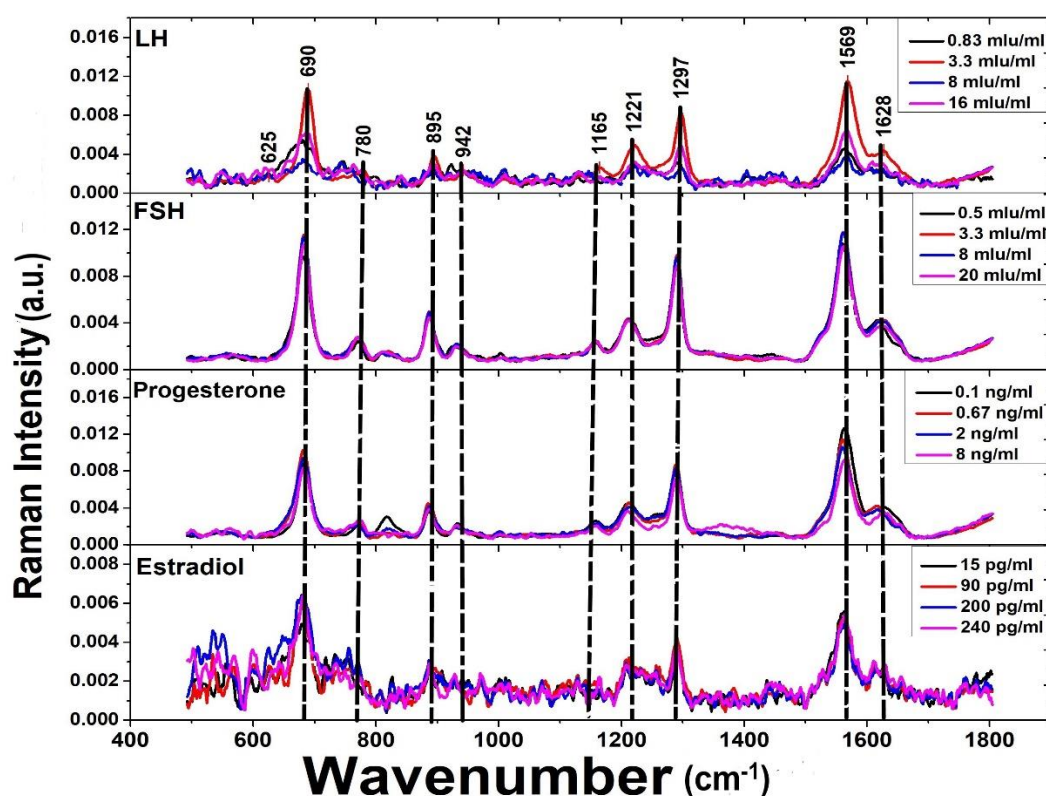


Figure 5. 4: Average characteristic Raman spectra of selected concentrations of female reproductive hormones standards FSH, LH, Estradiol, and Progesterone mixed with male Wistar rat's blood.

The Raman spectra were found to have almost identical profiles structure as expected since all the hormones studied here are present naturally in the blood (Barp *et al.*, 2002).

Variations were observed in the intensity of bands centered around wavenumbers 690, 895, 1165, 1221, 1297, 1559 and 1628 cm^{-1} in Luteinizing hormone, 1297, 1569 and 1628 cm^{-1} in Follicle Stimulating hormone, 780, 1221, 1297, 1659 and 1628 cm^{-1} in Progesterone and 690, 895 and 1221 cm^{-1} in Estradiol hormone. The tentative component and vibrational assignment of the Raman bands together with the references have been tabulated in Table 5.1

Table 5. 1: Prominent Raman bands in Raman spectra of the standard hormones (LH, FSH, Progesterone, and Estradiol) when mixed with male Wistar rat's blood, the tentative component and vibrational assignment of the bands together with the references.

Wavenumber/cm ⁻¹		Standard Hormones				Tentative Vibrational Assignment	References
EXPTAL	LIT.	LH	FSH	PRO	EST		
425	433	✓				C-H stretching of glucose	(Minaeva <i>et al.</i> , 2008)
541	542	✓				CH deformation	(Vedad <i>et al.</i> , 2018)
648	647			✓	✓	C-H out of the plane of Tyrosine	(Herrero, 2008, Dingari <i>et al.</i> , 2012)
679/699	680				✓	O-H vibrations with ring deformation	(Bright <i>et al.</i> , 2010)
756	750	✓		✓	✓	Tryptophan	(Ullah <i>et al.</i> , 2019, Herrero, 2008)
836/854	830		✓		✓	Tyrosine	(Davidson <i>et al.</i> , 2013, Jenkins <i>et al.</i> , 2005)
942	937			✓		C-C stretching of Phenylalanine	(Davidson <i>et al.</i> , 2013, Dingari <i>et al.</i> , 2012, Jenkins <i>et al.</i> , 2005)
969/972	965		✓			C-C stretching of Phenylalanine	(Dingari <i>et al.</i> , 2012), (Jenkins <i>et al.</i> , 2005)
1004			✓		✓	C-C stretching	(Dingari <i>et al.</i> , 2012)
1044	1040			✓		Cyclic alkyl ethers, C-C stretch	(Ilaslan <i>et al.</i> , 2015, Davidson <i>et al.</i> , 2013)
1125	1127				✓	C-C stretch of Protein	(Goeller and Riley, 2007, Potcoava <i>et al.</i> , 2014)

1221	1230	✓	✓	✓	✓	Amide III CH bend	(Goeller and Riley, 2007, Herrero, 2008)
1295/1297	1294		✓			CH ₂ twisting	(Bright <i>et al.</i> , 2010)
1354	1357	✓				Tryptophan	(Herrero, 2008)
1430	1448	✓				CH ₂ /CH ₃ deformation of protein	(Davidson <i>et al.</i> , 2013)
1479	1481			✓		CH external deformation	(Minaeva <i>et al.</i> , 2008)
1567/1569	1578			✓		C=C stretching of a protein molecule	(Goeller and Riley, 2007)
1656	1675			✓	✓	C=C stretching of Amide I	(Vedad <i>et al.</i> , 2018, Herrero, 2008)

Principal Component Analysis was performed on the spectral data set of standard solutions of female reproductive hormones (Follicle-stimulating hormone, Luteinizing hormone, Progesterone, and Estradiol) mixed with male Wistar rat's blood. This was done to segregate between Raman data sets of different concentrations in blood for each of the hormones. The bands exhibiting significant variance were utilized in the segregation by PCA and displayed as having larger signals in the Principal Component (PC) loadings plot displayed in figure 5.6.

Here, PCA was applied on a combined data set of different concentrations of standard solutions of female reproductive hormones mixed with male Wistar blood of Follicle Stimulating hormone (0.5-50 mlu/ml), Progesterone hormone (0.1-26.6 ng/ml), Luteinizing hormone (0.5-50 mlu/ml) and Estradiol (15-400 pg/ml). This analysis was performed in R software.

Figure 5.5 displays 3D PCA score plots of the four hormones with different concentration clusters. As displayed in the score plots for (Luteinizing hormone, Follicle Stimulating Hormone, Progesterone, and Estradiol), the different concentrations were appreciably segregated showing the power of Raman spectroscopy in level concentration variation detection.

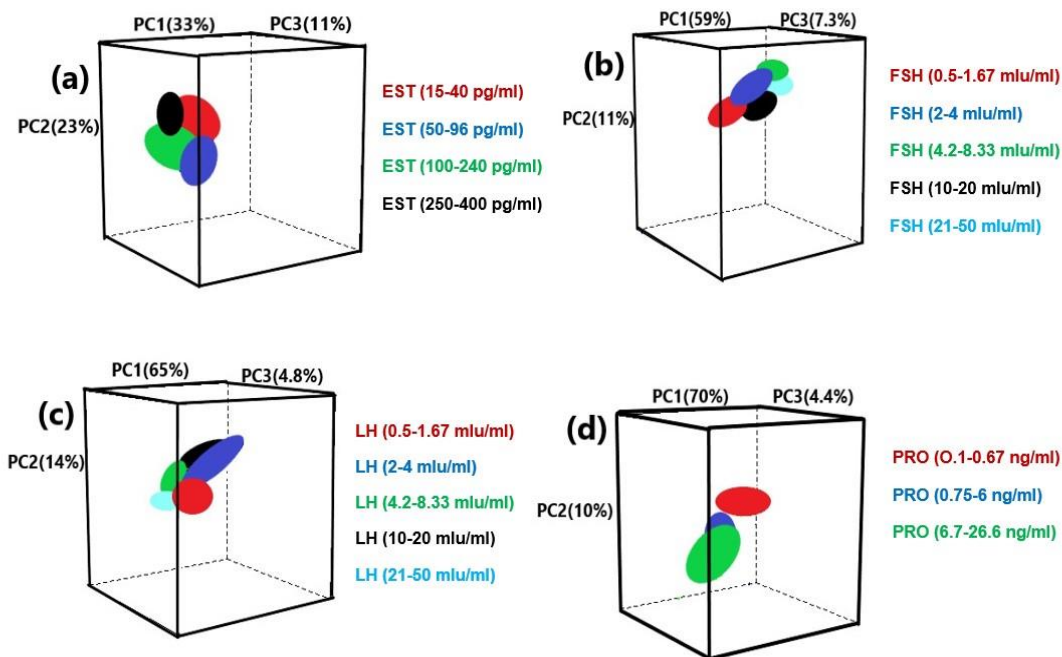


Figure 5. 5: PCA 3D score plot of Raman spectral data set of (a) Estradiol, (b) Follicle Stimulating hormone, (c) Luteinizing hormone, and (d) Progesterone hormone mixed with male Wistar rat's blood.

To identify the bands responsible for the segregation, the PCA loadings plots for the four hormones were also done and are displayed in figure 5.6. Concentrations of Luteinizing hormone (0.83, 2.5, 6.25 and 16 mlu/ml), Follicle Stimulating hormone (0.5, 3.3, 8.0 and 20 mlu/ml), Progesterone (0.1, 0.67, 2 and 8 ng/ml) and Estradiol hormone (15, 90, 200 and 240 pg/ml) were selected for the loadings plots for each of the hormones. This enabled us to identify the Raman biomarker for each hormone using Principal Component Analysis (PCA) that has been marked out in figure 5.6 below.

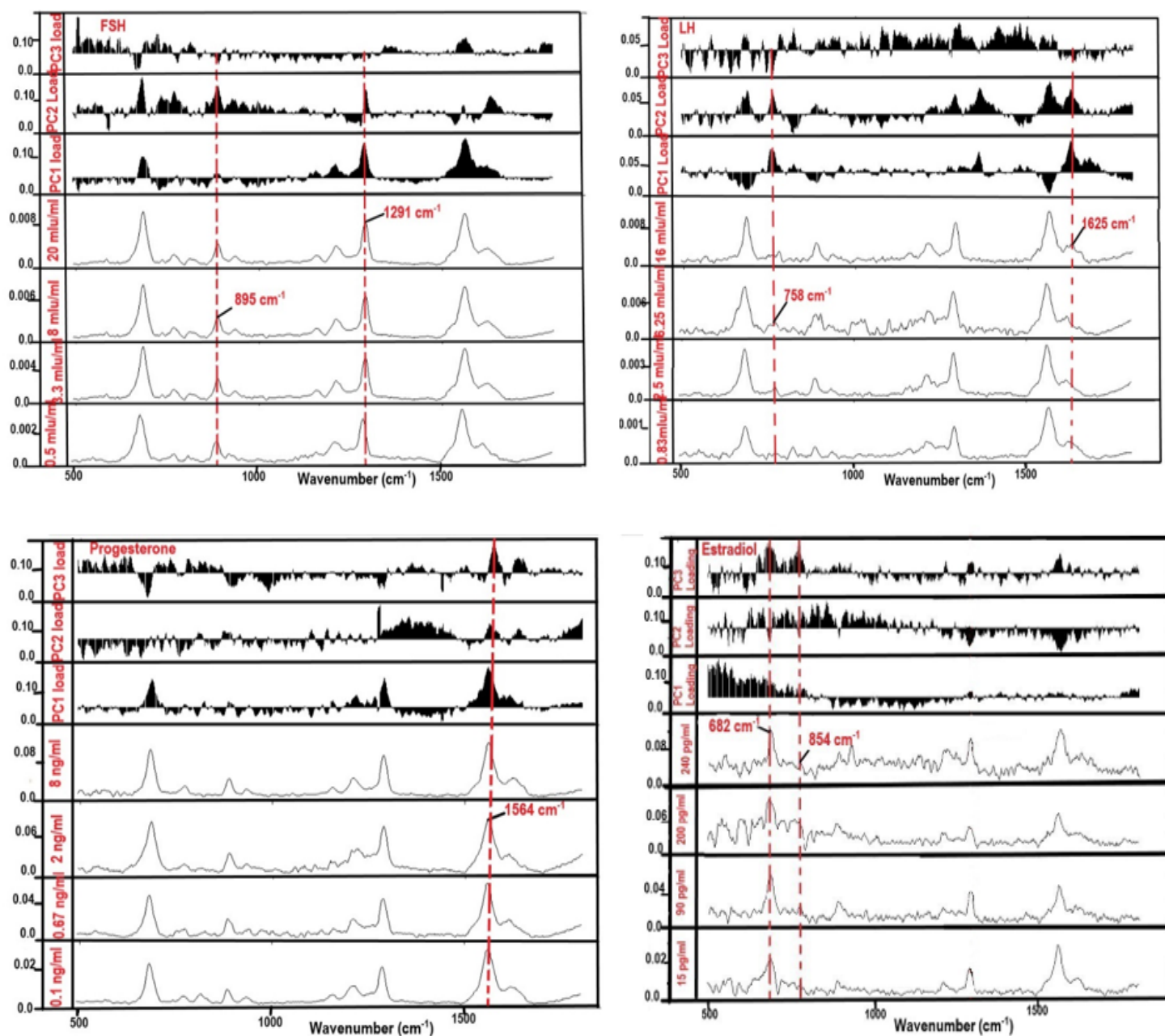


Figure 5.6: Loadings plots together with Raman spectra of FSH, LH, Progesterone, and Estradiol hormone mixed with male Wistar rat's blood.

From the Loadings plots, the bands exhibiting significant intensity variation with concentrations were centered at wavenumbers; 758 and 1625 cm^{-1} for Luteinizing hormone (LH), 895, and 1291 cm^{-1} for Follicle Stimulating Hormone (FSH), 682 and 854 cm^{-1} for Estradiol hormone, and 1564 cm^{-1} for progesterone hormone. These bands could be used as unique biomarkers for the respective hormones in the blood.

5.4 Raman Spectra of blood samples obtained from normal (untreated), *Asparagus racemosus* (herbal extract), and ibuprofen treated female Wistar rats.

The spectra of blood samples obtained from female rats were studied in detecting the level of hormonal variation in the animal subjects. Female Wistar rats were treated with *Asparagus racemosus* (herbal extract) traditionally known as a fertility and pain relief plant and also used to treat illnesses like diabetes, aging prevention, female reproductive disorders and to increase milk production in nursing mothers (College, 2013) and ibuprofen administered for pain relief. This herbal plant has been known for its great benefits in improving overall health especially the female reproductive system (Sharma, 2011) compared to the effects of the conventional pain killer drug ibuprofen.

The levels of the female reproductive hormones were expected to vary upon the administration of these drugs. *Asparagus racemosus* is traditionally used to influence fertility in women while Ibuprofen is used for pain relief from primary dysmenorrhea (August *et al.*, 2017).

Figure 5.7 shows the obtained Raman spectra from the blood of normal (NRM), *Asparagus racemosus*-treated at a low dose (LD, 300 mg/Kg weight) and high dose (HD, 600 mg/Kg weight) together with ibuprofen-treated (IBU) female Wistar rats.

Using Analysis of Variance (ANOVA) to identify significant differences in the data, the collected data exhibited significant variance in the days (Day 3,7 and 11) through descriptive statistics. This enabled us to study the variations in the hormones at the beginning of the study represented by Day 3, midway the study represented by Day 7, and the end of the study represented by Day 11.

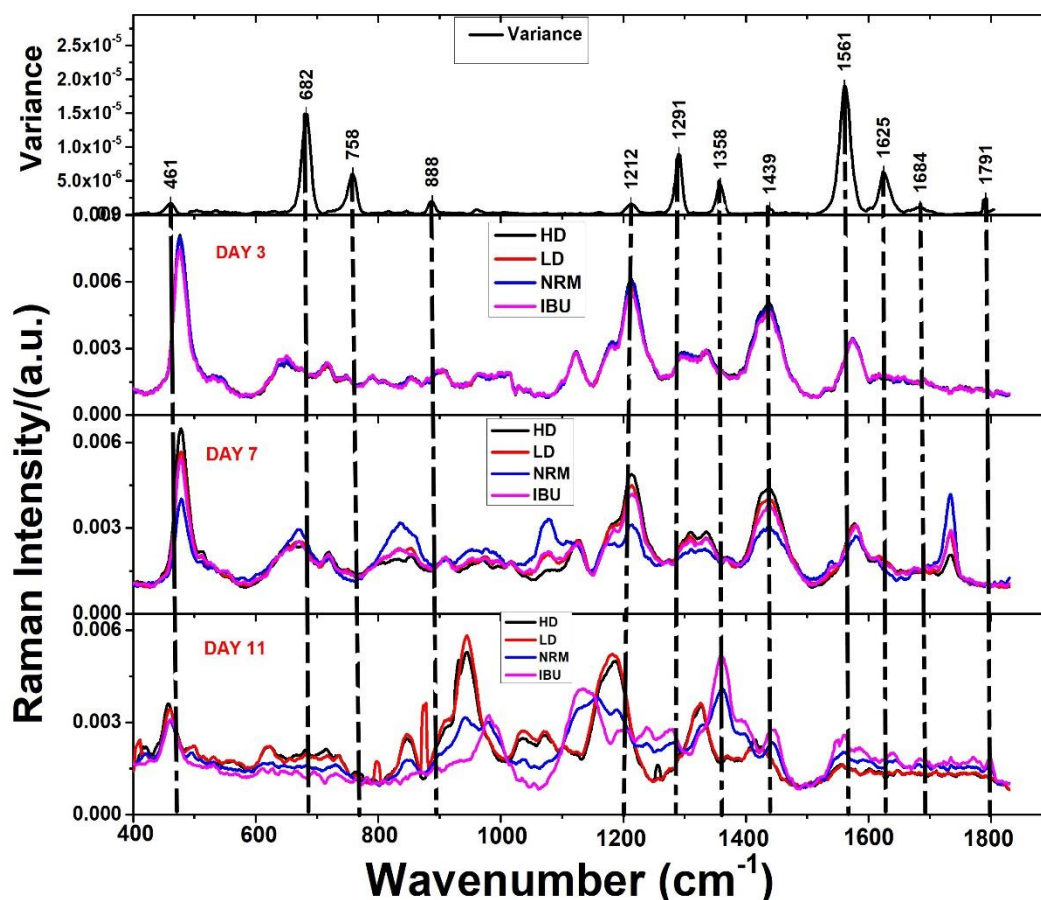


Figure 5. 7: Raman spectra of the blood samples for the untreated (normal saline), High and Low doses of *Asparagus racemosus* together with the Ibuprofen treated female Wistar rats on day 3, 7, and 11 with variance.

KEY

HD - High dose of *Asparagus racemosus*

LD - Low dose of *Asparagus racemosus*

NRM - Normal saline (control)

IBU - Ibuprofen

The variance was calculated in excel across all the spectral data obtained from both blood and vaginal fluid samples during this study. The same variance was used for both blood and vaginal fluid samples for a better comparison of the influence of *Asparagus racemosus* (herbal extract) and ibuprofen on female reproductive hormones in the blood and vaginal fluid samples. The biomarkers Raman bands identified earlier in this work were among the Raman bands found to exhibit high variance values in the variance curve.

These bands were those centered at wavenumbers 1625 cm^{-1} for Luteinizing hormone, 1561 cm^{-1} for progesterone, 1291 cm^{-1} for Follicle Stimulating Hormone, and 682 cm^{-1} of Estradiol displayed in figures 5.7, 5.1, and 5.4. These bands were also identified using the loadings plots in Principal Component Analysis (PCA) as displayed in figure 5.6. Other Raman bands identified in the variance spectrum other than the Raman biomarker bands were centered at $461, 758, 888, 1212, 1439, 1684,$ and 1791 cm^{-1} .

The biomarker Raman bands for the respective hormones were used in studying the influence of the two doses of *Asparagus racemosus* and Ibuprofen on the female reproductive hormones of the female Wistar rats.

Figure 5.8 below shows plots of the average intensity of the respective hormone biomarker bands versus the animal groups that is the normal (untreated) and treated animals at the selected days (day 3,7 and 11) with the error bar. The influence of the treatments on the hormones as extracted from the plots in figure 5.7 has been summarised in figure 5.8 and table 5.2.

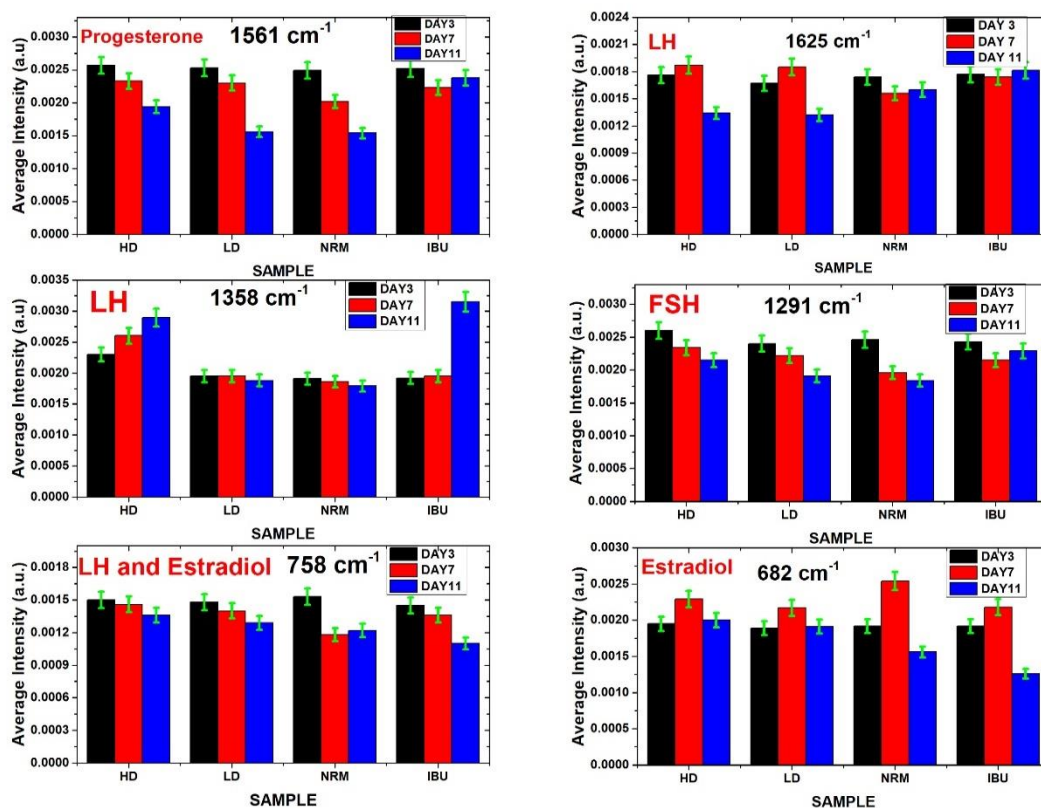


Figure 5. 8: Plots of Average intensity versus animal groups (treated and normal) for the selected days (Day 3,7 and 11).

Figure 5.8 shows the Influence of *Asparagus racemosus* and Ibuprofen treated together with normal saline (untreated) on the female reproductive hormones in blood samples of Wistar rats which are evident and this has been achievable with Raman spectroscopic technique.

The variation in the intensity of the identified biomarker Raman spectral bands indicates the level variation of the respective hormone in the blood of the different animal subject groups. This was due to the interaction of *Asparagus racemosus* (herbal extract) and Ibuprofen with the reproductive hormones in managing dysmenorrhea and cyclicity patterns of the menstrual cycle to create a balance. The significant variation shows the effect of *Asparagus racemosus* and Ibuprofen on the reproductive hormones in the management of dysmenorrhea (menstrual pains) (Kaaria *et al.*, 2019, Karimi *et al.*, 2018).

5.5 Raman Spectra of vaginal fluid obtained from female Wistar rats treated with *Asparagus racemosus* (herbal extract) and ibuprofen.

A possibility of detecting a similar hormonal variation observed in blood samples from the animals was also investigated on the vaginal fluid samples upon application onto conductive silver smeared substrates. Since the vaginal fluid is non-invasively obtained, this may become an interesting avenue for hormonal variation investigations if it works with Raman spectroscopy.

As shown in figure 5.9, the profile of the variance curve obtained across the Raman spectra of blood and vaginal fluid samples collected for fourteen days was used and this enabled us to compare the results obtained from the two different samples of the subject animals.

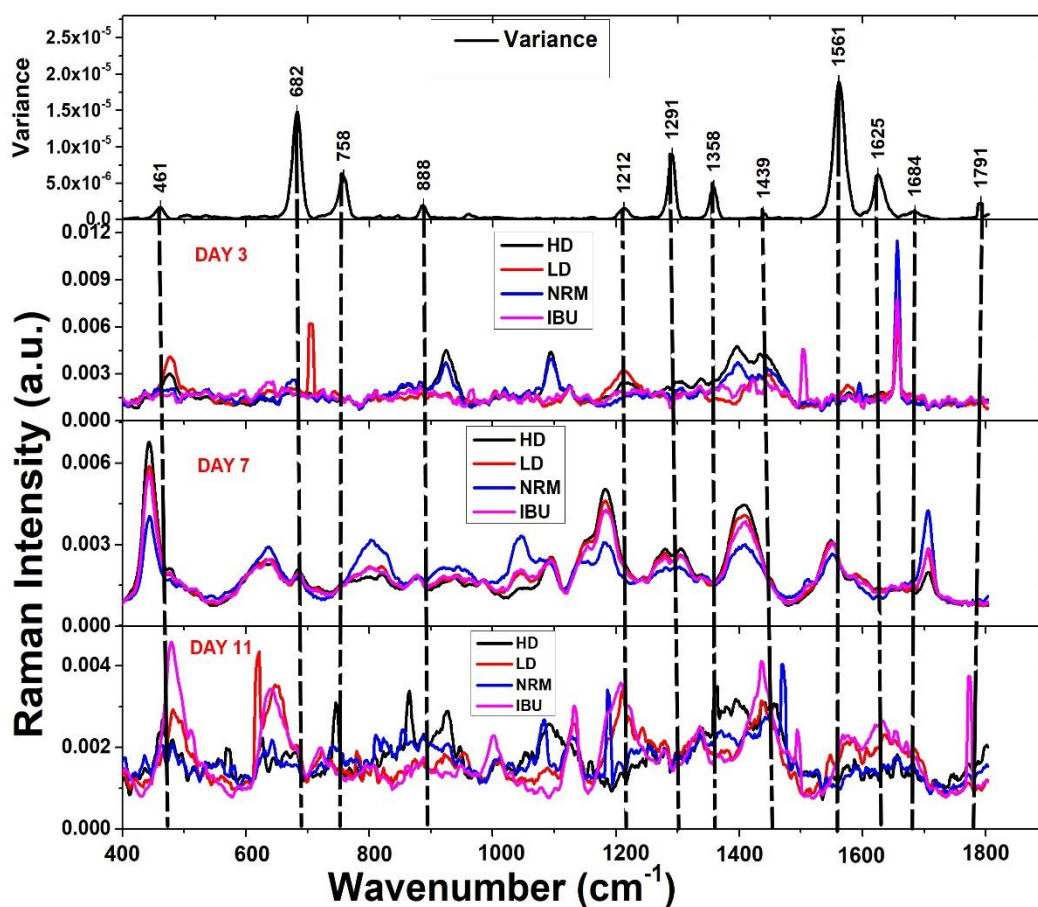


Figure 5. 9:Raman spectra of the vaginal fluid samples for the nontreated (normal saline), High and Low doses of *Asparagus racemosus* together with the Ibuprofen treated female Wistar rats on day 3, 7, and 11 with variance.

The plots of the average intensity of the Raman biomarker bands for each hormone against animal groups (*Asparagus racemosus* treated, Ibuprofen treated, and the untreated) for days 3,7 and 11 are shown in Figure 5.10.

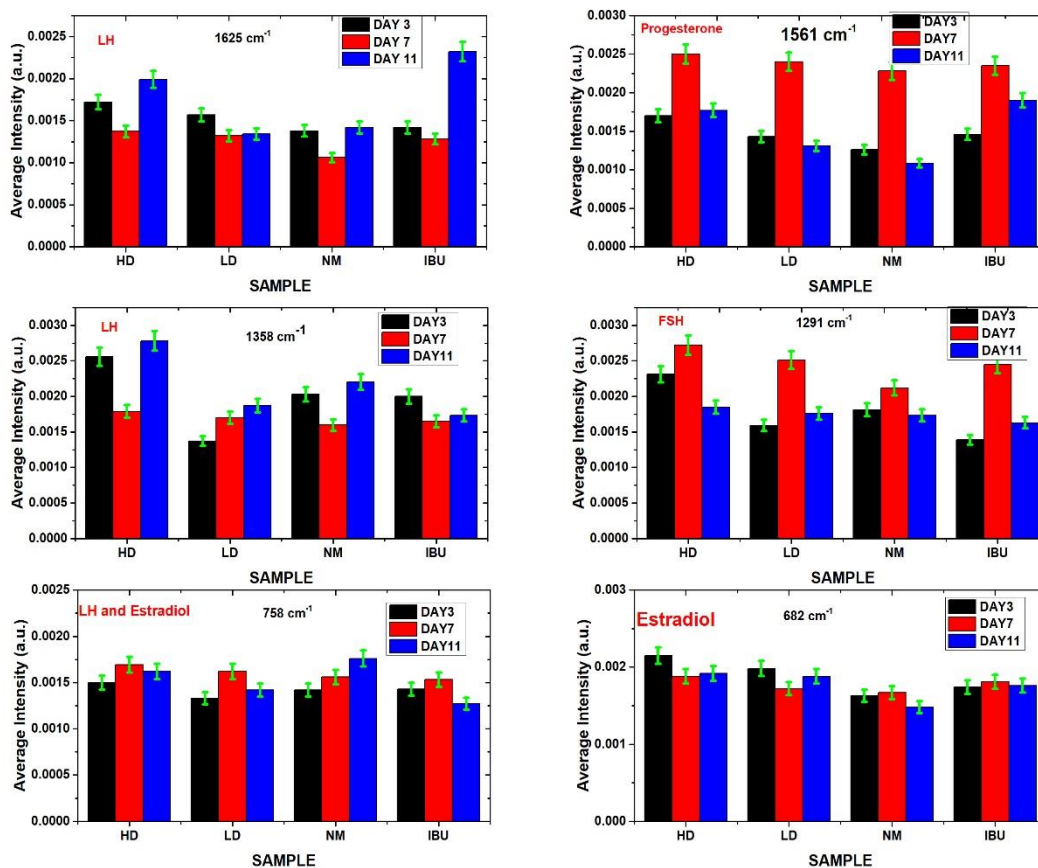


Figure 5. 10: Plots of Average intensity versus animal groups (treated and normal) for the selected days (Day 3,7, and 11).

With Raman spectroscopic technique, a similar influence of *Asparagus racemosus* (herbal extract) and ibuprofen on the female reproductive hormones is observed in both blood and vaginal fluid samples for day 3, day 7, and day 11 for the Raman biomarker bands (1291 cm⁻¹ for Follicle Stimulating hormone, 1625 cm⁻¹ for Luteinizing hormone, 682 cm⁻¹ for Estradiol and 1561 cm⁻¹ for Progesterone hormone) that were identified for each reproductive hormone.

The summary of the influence of *Asparagus racemosus* (herbal extract) and ibuprofen on female reproductive hormones in the blood and vaginal fluid samples obtained from the same subject animals were tabulated in table 5.2 below.

Table 5. 2: Influence of Ibuprofen, normal Saline (control), and different doses of *Asparagus racemosus* on the female reproductive hormones in Wistar rats.

Wavenumber /cm ⁻¹	Standard hormones	Day	Blood	Vaginal fluid
682	Estradiol	11	HD had a great influence on the hormone followed by LD, then NRM, and least IBU	HD had a great influence on the hormone followed by LD, then IBU, and least NRM
		7	NRM had a great influence on the hormone followed by HD, then IBU, and least LD	IBU had a great influence on the hormone followed by HD, then NRM, and least LD
		3	HD had a great influence on the hormone followed by IBU, then NRM, and least LD	HD had a great influence on the hormone followed by LD, then IBU, and least LD
758	Estradiol and Luteinizing hormone LH	11	HD had a great influence on the hormones followed by LD, then NRM, and least IBU	NRM had a great influence on the hormones followed by HD, then LD, and least IBU
		7	HD had a great influence on the hormones followed by LD, then IBU, and least NRM	HD had a great influence on the hormones followed by LD, then IBU, and least NRM
		3	NRM had a great influence on the hormones followed by HD, then LD, and least IBU	HD had a great influence on the hormones followed by IBU, then NRM, and least LD
1291	Follicle Stimulating hormone FSH	11	IBU had a great influence on the hormone followed by HD, then LD, and least NRM	HD had a great influence on the hormone followed by LD, then IBU, and least NRM
		7	HD had a great influence on the hormone followed by LD, then IBU, and least NRM	HD had a great influence on the hormone followed by LD, then IBU, and least NRM
		3	HD had a great influence on the hormone followed by NRM, then LD, and least IBU	HD had a great influence on the hormone followed by NRM, then LD, and least IBU

1358	Luteinizing hormone LH	11	IBU had a great influence on the hormone followed by HD, then LD, and least NRM	HD had a great influence on the hormone followed by NRM, then LD, and least IBU
		7	HD had a great influence on the hormone followed by LD, then IBU, and least NRM	HD had a great influence on the hormone followed by IBU, then NRM, and least LD
		3	HD had a great influence on the hormone followed by LD, then IBU, and least NRM	HD had a great influence on the hormone followed by IBU, then NRM, and least LD
1561	Progesterone	11	IBU had a great influence on the hormone followed by HD, then LD, and least NRM	IBU had a great influence on the hormone followed by HD, then LD, and least NRM
		7	HD had a great influence on the hormone followed by LD, then IBU, and least NRM	HD had a great influence on the hormone followed by LD, then IBU, and least NRM
		3	HD had a great influence on the hormone followed by LD, then IBU, and least NRM	HD had a great influence on the hormone followed by LD, then IBU, and least NRM
1625	Luteinizing hormone LH	11	IBU had a great influence on the hormones followed by NRM, then HD, and least LD	IBU had a great influence on the hormones followed by HD, then NRM, and least LD
		7	HD had a great influence on the hormones followed by LD, then IBU, and least NRM	HD had a great influence on the hormones followed by LD, then IBU, and least NRM
		3	HD had a great influence on the hormones followed by IBU, then NRM, and least LD	HD had a great influence on the hormones followed by LD, then IBU, and least NRM

From table 5.2, the treatments (*Asparagus racemosus* and Ibuprofen) influenced the reproductive hormones differently. Almost a similar influence on the hormones was noticed on day 7 in both blood and the vaginal fluid samples. *Asparagus racemosus* had great influence as compared to ibuprofen and normal saline (control) on the female reproductive hormones across the study. *Asparagus racemosus* greatly influenced the levels of Estradiol and Luteinizing hormone than Progesterone and Follicle Stimulating hormone (Karimi *et al.*, 2018). *Asparagus racemosus* has been administered as a pain relief and fertility plant due to the different compounds (glycosides, flavonoids, saponins, and terpenoids) it contains. These compounds increase the levels of Estradiol hormone which is very fundamental in improving the chances of conception and reducing pain (Kumar and Singh, 2001). Maximum influence on the reproductive hormones was observed with the high dose (600 mg/Kg weight) of *Asparagus racemosus*.

The levels of Estradiol usually increase to create a balance during the management of menstrual pains (primary dysmenorrhea) as it has been observed during this study which is in agreement with what has been reported (Vincent and Tracey, 2008).

Ibuprofen caused the levels of reproductive hormones to reduce. This is because ibuprofen inhibits the biosynthesis of endometrial prostaglandin $F_{2\alpha}$ ($PGF_{2\alpha}$) by reducing the menstrual fluid when managing primary dysmenorrhea hence relieving the menstrual pain (Dawood and Khan-Dawood, 2007).

5.6 Quantification of hormones using Artificial Neural Networks (ANN)

5.6.1 Quantification of the standard solutions of the female reproductive hormones mixed with male Wistar rat's blood.

To quantify the concentration of hormones in blood based on Raman spectral data, an additional analysis is needed to extract this information. In this work, Artificial Neural Networks models of three layers for each female reproductive hormone (FSH, LH, Estradiol, and Progesterone) were developed using the resilient backpropagation neural network for the data obtained from samples prepared by mixing solutions of standard hormones with male Wistar rat's blood which does not contain any female reproductive hormones.

The spectral region around the Raman biomarker band for each hormone (1291 cm^{-1} for Follicle Stimulating Hormone, 1625 cm^{-1} for Luteinizing hormone, 1564 cm^{-1} for Progesterone, and 682 cm^{-1} for Estradiol) was used to develop an ANN model for each hormone.

The ANN models were developed using R software, the calibration and test values of Mean Absolute Error, Root Mean Square Error, and Determination coefficient were calculated and used to test the accuracy of the model. The values for each hormone have been tabulated in Table 5.3 below. The values obtained for MAE and RSME were very low while the values of R^2 were approximately equal to one implying there is a correlation between the actual concentration values and the predicted concentration values hence great accuracy. The values of MAE, RSME, and R^2 were tabulated in table 5.3 below.

Table 5. 3: ANN validation results for each of the models developed for standard solutions of Follicle Stimulating Hormone, Luteinizing hormone, Progesterone, and Estradiol mixed with male Wistar rat's blood.

STANDARD HORMONES	Number of calibration and test samples	MAE		RSME		R^2	
		Calibration	Test	Calibration	Test	Calibration	Test
FSH (mlu/ml)	15 calibration	0.0189	0.0079	0.0483	0.0390	0.9943	0.9674
	28 test samples						
LH (mlu/ml)	15 Calibration	0.0124	0.0284	0.0241	0.0125	0.9984	0.9863
	28 test samples						
Estradiol (pg/ml)	15 calibration	0.0176	0.0055	0.0195	0.0163	0.9989	0.9791
	22 test samples						
Progesterone (ng/ml)	15 calibration	0.0677	0.0167	0.0172	0.0286	0.9969	0.9858
	18 test samples						

Regression plots for the ANN models of the four female reproductive hormones were accurate since the actual concentration and the predicted concentration values were able to make the regression line of the models developed implying good performance of the model. Below are regression plots for each of the four reproductive hormones.

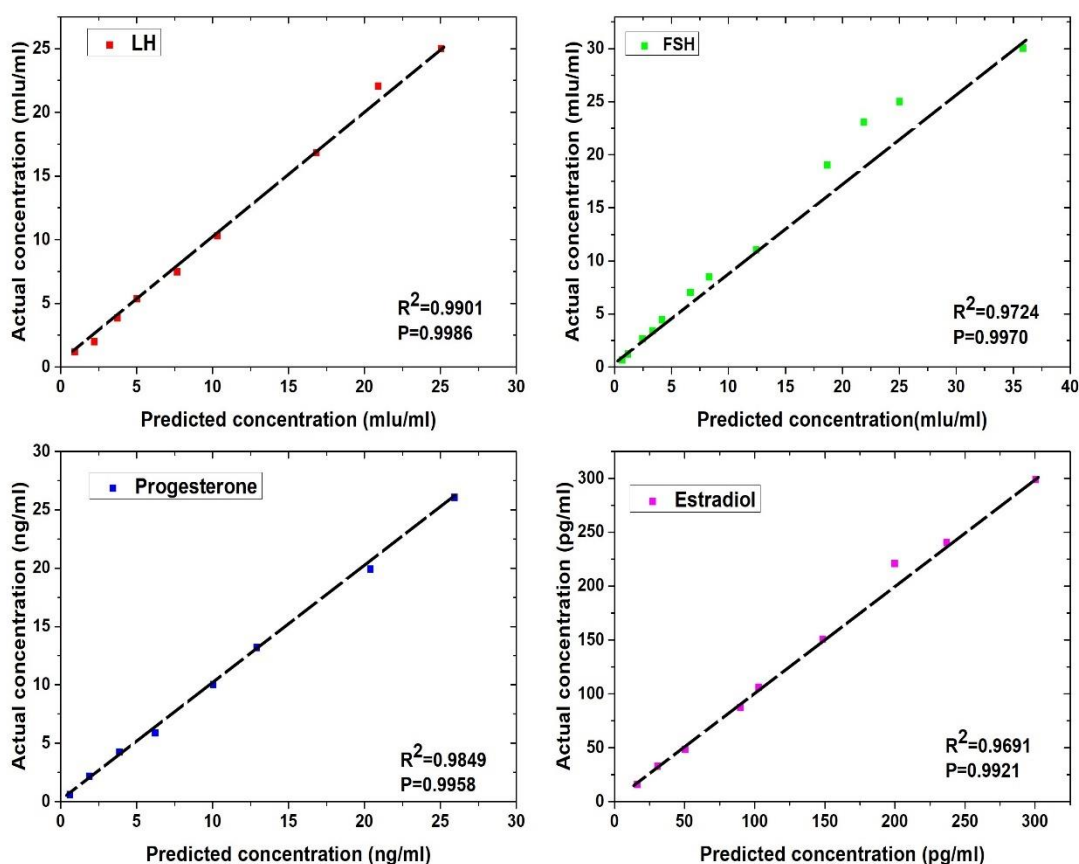


Figure 5. 11: ANN regression plots for Luteinizing Hormone, Follicle Stimulating Hormone, Estradiol, and Progesterone.

5.6.2 Limit of Detection (LOD)

The ANN models developed using the Raman spectral data obtained when the standard solutions of the female reproductive hormones were mixed with male Wistar rat's blood were evaluated to determine the Limit of Detection (LOD). The LOD for each hormone was calculated with references to the Raman biomarker bands using the equation below (Dingari *et al.*, 2012);

$$LOD = K \frac{\sigma_B}{S} \quad (5.1)$$

Where;

K is the expansion factor approximately equal to 3 and it depends on the acceptable false-negative error values (β) and false-positive error numbers (α).

S is the slope of the graph (ANN regression plot for each hormone) and

σ_B is the standard deviation of black signals which is the measure of the average deviation of the predicted values from the regression line given by the equation below (Dingari *et al.*, 2012);

$$\sigma_B = \left[\frac{\sum_i (C_p - C_r)^2}{N-2} \right]^{\frac{1}{2}} \quad (5.2)$$

Where;

C_p is the predicted concentration, C_r is the reference concentration and N is the number of spectra in the data set.

Using equation (5.1), the values for the Limit of Detection of each hormone were calculated and tabulated in Table 5.4 below.

Table 5. 4: Limit of Detection values in the Raman spectra of the standard hormones (LH, FSH, Progesterone, and Estradiol) when mixed with male Wistar rat's blood, literature values together with the references.

Female reproductive hormones	Limit of Detection		References
	Experimental	Literature	
Follicle Stimulating hormone (mlu/ml)	2.126	10 (HPLC)	(Robertson <i>et al.</i> , 2001)
Luteinizing hormone (mlu/ml)	2.494	10 (HPLC)	(Robertson <i>et al.</i> , 2001)
Progesterone (pg/ml)	8.31×10^3	2×10^5 (ELISA)	(Khatun <i>et al.</i> , 2009)
Estradiol (ng/ml)	8×10^{-3}	$2 \times 10^{-2} - 4.2 \times 10^{-2}$ (HPLC) 1.0×10^{-2} (ELISA)	(Kumar <i>et al.</i> , 2014), (Xu <i>et al.</i> , 2015)

The values obtained for the Limit of Detection (LOD) from the experimental data indicate that Raman spectroscopy has much better detection ability as compared to what has been reported in the literature with the conventional detection techniques.

5.6.3 Quantification of the Raman Spectra of blood from normal(nontreated), *Asparagus racemosus*, and ibuprofen treated female Wistar rats.

The ANN models that were developed using the standard solutions of the female reproductive hormones were trained to predict the concentrations of each female reproductive hormone in the Raman spectra obtained for days 3,7 and 11. Regarding the Raman biomarkers (1291 cm^{-1} for Follicle Stimulating Hormone, 1625 cm^{-1} for Luteinizing hormone, 1564 cm^{-1} for Progesterone, and 682 cm^{-1} for Estradiol), the obtained Raman spectra for day 3,7 and 11 were fed into each model that was developed. Each model was able to predict the values of the concentrations for each hormone which have been summarized in table 5.4 below.

Table 5. 5: Concentration levels of the female reproductive hormone in the blood of days 3,7 and 11 for *Asparagus racemosus* treated, Ibuprofen treated, and the nontreated (normal saline) female Wistar rats.

Treat ment days	FSH/ mlu/ml				LH/ mlu/ml			
	HD	LD	NRM	IBU	HD	LD	NRM	IBU
Day 3	3.61±0.81	3.52±0.76	3.56±0.78	3.46±0.74	8.82±0.44	8.79±0.43	8.74±0.43	8.64±0.43
Day 7	3.83±0.81	3.72±0.76	3.67±0.78	3.69±0.74	8.88±0.44	8.85±0.43	8.79±0.43	8.95±0.43
Day 11	3.71±0.81	3.68±0.76	3.6±0.78	3.63±0.74	8.7±0.44	8.62±0.43	8.67±0.43	8.5±0.432
Mean	3.71±0.186	3.64±0.182	3.61±0.181	3.6±0.18	8.8±0.44	8.75±0.437	8.73±0.43	8.7±0.435
Treat ment days	Progesterone /ng/ml				Estradiol/ pg/ml			
	HD	LD	NRM	IBU	HD	LD	NRM	IBU
Day 3	13.73±0.687	13.69±0.684	13±0.65	13.44±0.672	120.82±6.04	116.54±5.83	115.13±5.76	116.97±5.85
Day 7	13.43±0.687	13.37±0.684	13.21±0.65	13.3±0.672	119.49±6.04	117.21±5.83	116.34±5.76	118.01±5.85
Day 11	13.12±0.687	12.99±0.684	12.95±0.65	13.16±0.672	119.69±6.04	118.43±5.83	117.07±5.76	116.97±5.85
Mean	13.43±0.672	13.35±0.665	13.05±0.653	13.3±0.665	120.0±6.0	117.39±5.87	116.18±5.81	117.32±5.87

KEY

HD -High dose of *Asparagus racemosus* **LD** -Low dose of *Asparagus racemosus*

NRM - Normal saline (control) **IBU** -Ibuprofen

From table 5.5, we notice that compared to the normal (untreated), *Asparagus racemosus* (herbal extract) caused an elevation in the levels of the female reproductive hormones (Follicle Stimulating Hormone, Luteinizing hormone, Progesterone, and Estradiol) with high dose having a greater effect than the low dose as compared to the normal (untreated). Ibuprofen reduced the levels of the female reproductive hormones as compared to the normal.

Percentage deviations from the normal (untreated) of *Asparagus racemosus* (herbal extract) and ibuprofen treated of each of the average concentrations for day 3,7, and 11 for the female reproductive hormones (FSH, LH, Progesterone, and Estradiol) have been calculated and tabulated in Table 5.6 below.

Table 5. 6: Percentage deviation of Asparagus racemosus (herbal extract) and ibuprofen treated from the normal (untreated).

Female reproductive hormones	Percentage deviation from the normal (untreated) (%)		
	HD	LD	IBU
FSH	+5.2	+5.1	-5
LH	+5	+5	-4.9
Progesterone	+5.1	+5	+5
Estradiol	+5.2	+5.1	+5.1

During the management of primary dysmenorrhea (menstrual pains) with *Asparagus racemosus* (herbal extract), the levels of the female reproductive hormones are expected to increase and with Ibuprofen the levels of these hormones decrease hence affecting fertility (Vincent and Tracey, 2008). The influence can also be noticed with the average concentration levels for each hormone were calculated across day 3, 7, and 11 that was also displayed in table 5.5. This is in agreement with the information displayed in figures 5.8 and 5.10.

The chemometric analysis tools (Principal Component Analysis and Artificial Neural Networks) used to validate and quantify the results obtained from the subject animals were able to give the same findings on the influence of *Asparagus racemosus* (herbal extract) and Ibuprofen on the female reproductive hormones (Follicle Stimulating Hormone, Luteinizing hormone, progesterone, and Estradiol).

CHAPTER 6: CONCLUSION AND RECOMMENDATION

6.1 Conclusion

Raman Spectroscopy technique in the study of hormonal variability yielded good results and hormonal variations were detected in the female reproductive hormones in female Wistar rats. This research has shown that hormonal variation is detectable in both blood and the vaginal fluid samples using Raman Spectroscopy in Wistar rats as shown from the results obtained.

The spectral profiles obtained from Wistar rats' blood and vaginal fluid samples revealed variations in the female reproductive hormone (FSH, LH, Progesterone, and Estradiol) when *Asparagus racemosus* (herbal extract) and ibuprofen treated as compared to the normal (untreated).

Raman spectroscopy technique was able to identify vibrational bonds for the standard solutions of the female reproductive hormones and the standard solutions mixed with male Wistar rat's blood. The Raman biomarker bands were centered at 1625 cm^{-1} for the Luteinizing hormone, 1291 cm^{-1} for Follicle Stimulating hormone, 1564 cm^{-1} for Progesterone, and 682 cm^{-1} for Estradiol hormone.

With the Raman Spectroscopy, it has been shown that *Asparagus racemosus* (herbal extract) had the greatest influence on the reproductive hormone than ibuprofen. With *Asparagus racemosus* (herbal extract), a greater effect was observed with a high dose than a low dose.

Raman Spectroscopy Technique can be preferred to the traditional conventional methods (ELISA, HPLC, Mass spectroscopy, Electrophoresis) that are very expensive, require much sample preparation hence time-consuming, do not give instant results and the results obtained are subjective. Raman Spectroscopy is highly sensitive, fast, reliable, non-invasive, and requires less sample preparation.

The main drawback of this approach is that results are not collected directly from the Raman Spectrometer so it is important to use other data mining techniques (chemometric tools) have to collect, process, analyze and interpret results from the collected spectral data.

Artificial Neural Networks (ANN) and Principal Component Analysis (PCA) chemometric tools were employed and provided good results through clustering and Raman biomarker in PCA and applying the developed ANN models for each reproductive hormone to predict the concentrations of the hormones that were fed in the ANN model for days 3,7, and 11.

It was found that compared to the untreated rats (Normal), administration of a high dose of *Asparagus racemosus* resulted in increased levels of FSH and estradiol by 5.2%, that of LH increased by 5% while that of progesterone increased by 5.2% in blood. Ibuprofen on the other hand was found to decrease FSH and progesterone by 5%, that of LH decreased by 4.9%, and that of estradiol by 5.1%.

The Limit of Detection (LOD) for the developed ANN models for each hormone was estimated as 2.126 mlu/ml, 2.494 mlu/ml, 8.31×10^3 ng/ml, and 8×10^{-3} pg/ml for FSH, LH, progesterone, and estradiol respectively. These LOD values were much lower than those reported for conventional detection techniques.

With the results obtained, the Raman Spectroscopy was a very effective analytical and detection technique that is fast, highly sensitive, and relatively affordable than the available conventional detection techniques which is a great insight in the medical sector for the detection of hormonal variation.

6.2 Recommendations

We recommend the use of different fluid samples like saliva on the same study of detecting hormonal variation and the influence of *Asparagus racemosus* (herbal extract) and ibuprofen on female reproductive hormones when administered in female Wistar rats.

This study can be done with human beings in exploring Raman Spectroscopy as a fast and sensitive detection and analytical technique for hormonal variation in the medical sector.

REFERENCES

- Abbott, L. C., Batchelor, S. N., Lindsay, J. R., and Moore, J. N. (2010). Resonance Raman and UV – visible spectroscopy of black dyes on textiles. *Forensic Sci. Int.* **202**, 54–63.
- Advis, J. P., Hernandez, L., and Guzman, N. A. (1989). Analysis of brain neuropeptides by capillary electrophoresis: determination of luteinizing hormone-releasing hormone from ovine hypothalamus. *Peptide Research*, **2**(6), 389.
- Agarwal, U. P., Ralph, S. A., Padmakshan, D., Liu, S., and Foster, C. E. (2019). Estimation of syringyl units in wood lignins by FT-Raman spectroscopy. *Journal of agricultural and food chemistry*, **67**(15), 4367-4374.
- Alok, S., Jain, S. K., Verma, A., Kumar, M., Mahor, A., and Sabharwal, M. (2013). Plant profile, phytochemistry, and pharmacology of *Asparagus racemosus* (Shatavari): A review. *Asian Pacific journal of tropical disease*, **3**(3), 242-251.
- Aretz, I., and Meierhofer, D. (2016). Advantages and pitfalls of mass spectrometry-based metabolome profiling in systems biology. *International journal of molecular sciences*, **17**(5), 632.
- Asensio, L., González, I., García, T., and Martín, R. (2008). Determination of food authenticity by enzyme-linked immunosorbent assay (ELISA). *Food control*, **19**(1), 1-8.
- August, J.-, Agbai, E. O., Eke, C. C., Nwanegwo, C. O., and Anyaehie, B. (2017). Comparison of the inhibitory effect of ibuprofen with *Piper guineense* Schumach and Thonn. on some reproductive hormones in female rats. *The Phytopharmacology*, **6**, 205–209.
- Auner, G. W., Koya, S. K., Huang, C., Broadbent, B., Trexler, M., Auner, Z., ... and Brusatori, M. A. (2018). Applications of Raman spectroscopy in cancer diagnosis. *Cancer and Metastasis Reviews*, **37**(4), 691-717.
- Barp, J., Araújo, A. S. D. R., Fernandes, T. R. G., Rigatto, K. V., Llesuy, S., Belló-Klein, A., and Singal, P. (2002). Myocardial antioxidant and oxidative stress changes due to sex hormones. *Brazilian Journal of Medical and Biological Research*, **35**(9), 1075-1081.
- Birech, Z., Mwangi, P. W., Bukachi, F., and Mandela, K. M. (2017). Application of Raman spectroscopy in type 2 diabetes screening in blood using leucine and isoleucine amino-acids as biomarkers and in comparative anti-diabetic drug efficacy studies. *PloS one*, **12**(9).

- Birech, Z., Ondieki, A. M., Opati, R. I., and Mwangi, P. W. (2020). Low-cost Raman sample substrates from conductive silver paint smear for Raman spectroscopic screening of metabolic diseases in whole blood. *Vibrational Spectroscopy*, 103063.
- Bright, A., Devi, T. R., and Gunasekaran, S. (2010). Spectroscopical vibrational band assignment and qualitative analysis of biomedical compounds with cardiovascular activity. *Int J Chem Tech Res*, 2(1), 379-388.
- Caligioni, C. S. (2009). Assessing reproductive status/stages in mice. *Current protocols in neuroscience*, 48(1), A-4I.
- Christensen, A., Bentley, G. E., Cabrera, R., Ortega, H. H., Perfito, N., Wu, T. J., and Micevych, P. (2012). Hormonal regulation of female reproduction. *Hormone and Metabolic Research*, 44(08), 587-591.
- Colah, R. B., Surve, R., Sawant, P., D'Souza, E., Italia, K., Phanasgaonkar, S., Nadkarni, A. H., and Gorakshakar, A. C. (2007). HPLC studies in hemoglobinopathies. *Indian J. Pediatr.* 74, 657–662.
- College, C. U. S. S. (2013). World Journal of Pharmaceutical research treatment. 2, 1466–1474.
- Corio, P., Andrade, G. F. S., Diógenes, I. C. N., Moreira, I. S., Nart, F. C., and Temperini, M. L. A. (2002). Characterization of the [Ru (CN) 5 (pyS)] 4⁻ ion complex adsorbed on gold, silver, and copper substrates by surface-enhanced Raman spectroscopy. *Journal of Electroanalytical Chemistry*, 520(1-2), 40-46.
- Craig, A. P., Franca, A. S., and Irudayaraj, J. (2013). Surface-enhanced Raman spectroscopy applied to food safety. *Annual review of food science and technology*, 4, 369-380.
- Duraipandian, S., Zheng, W., Ng, J., Lowe, J. J., Ilancheran, A., and Huang, Z. (2012, February). Effect of hormonal variation on in vivo high wavenumber Raman spectra improves cervical precancer detection. *Advanced Biomedical and Clinical Diagnostic Systems X* (Vol. 8214, p. 82140A). International Society for Optics and Photonics.
- Davidson, B., Murray, A. A., Elfick, A., and Spears, N. (2013). Raman micro-spectroscopy can be used to investigate the developmental stage of the mouse oocyte. *PloS one*, 8(7).
- Dawood, M. Y. (1984). Ibuprofen and dysmenorrhea. *The American journal of medicine*, 77(1), 87-94.

- Dawood, M. Y., and Khan-Dawood, F. S. (2007). Clinical efficacy and differential inhibition of menstrual fluid prostaglandin F_{2α} in a randomized, double-blind, crossover treatment with placebo, acetaminophen, and ibuprofen in primary dysmenorrhea. *American journal of obstetrics and gynecology*, **196**(1), 35-e1.
- Derntl, B., Pintzinger, N., Kryspin-Exner, I., and Schöpf, V. (2014). The impact of sex hormone concentrations on decision-making in females and males. *Frontiers in neuroscience*, **8**, 352.
- Dingari, N. C., Horowitz, G. L., Kang, J. W., Dasari, R. R., and Barman, I. (2012). Raman spectroscopy provides a powerful diagnostic tool for the accurate determination of albumin glycation. *PLoS One*, **7**(2).
- Dzsaber, S., Negyedi, M., Bernath, B., Gyüre, B., Fehér, T., Kramberger, C., ... and Simon, F. (2015). A Fourier transform Raman spectrometer with visible laser excitation. *Journal of Raman Spectroscopy*, **46**(3), 327-332.
- Faulds, K., Smith, W. E., Graham, D., and Lacey, R. J. (2002). Assessment of silver and gold substrates for the detection of amphetamine sulfate by surface-enhanced Raman scattering (SERS). *Analyst*, **127**(2), 282-286.
- Fini, A., Ospitali, F., Zoppetti, G., and Puppini, N. (2008). ATR/Raman and fractal characterization of HPBCD/progesterone complex solid particles. *Pharmaceutical Research*, **25**(9), 2030-2040.
- Gascon, J., Oubiña, A., and Barceló, D. (1997). Detection of endocrine-disrupting pesticides by enzyme-linked immunosorbent assay (ELISA): application to atrazine. *TrAC Trends in Analytical Chemistry*, **16**(10), 554-562.
- García, I., Sarabia, L. A., Ortiz, M. C., and Aldama, J. M. (2005). Optimization of the chromatographic conditions for the determination of hormones by gas chromatography with mass spectrometry detection. *Analytica Chimica Acta*, **544**(1-2), 26-35.
- Goeller, L. J., and Riley, M. R. (2007). Discrimination of bacteria and bacteriophages by Raman spectroscopy and surface-enhanced Raman spectroscopy. *Applied Spectroscopy*, **61**(7), 679-685.

- Grandi, G., Ferrari, S., Xholli, A., Cannoletta, M., Palma, F., Romani, C., ... and Cagnacci, A. (2012). Prevalence of menstrual pain in young women: what is dysmenorrhea? *Journal of pain research*, **5**, 169.
- Hahn, D. W. (2007). Raman scattering theory, Technical report. *Department of Mechanical and Aerospace Engineering, University of Florida*.
- Hale, J. E. (2013). Advantageous uses of mass spectrometry for the quantification of proteins. *International Journal of proteomics*, 2013.
- Hanson, B. A. (2012). ChemoSpec: Exploratory Chemometrics for Spectroscopy. *R package version*, 1-51.
- Heitman, L. H., Narlawar, R., de Vries, H., Willemsen, M. N., Wolfram, D., Brussee, J., and IJzerman, A. P. (2009). Substituted terphenyl compounds as the first class of low molecular weight allosteric inhibitors of the luteinizing hormone receptor. *Journal of medicinal chemistry*, **52**(7), 2036-2042.
- Herrero, A. M. (2008). Raman spectroscopy for monitoring protein structure in muscle food systems. *Critical reviews in food science and nutrition*, **48**(6), 512-523.
- Hosseini, S., Vázquez-Villegas, P., Rito-Palomares, M., and Martínez-Chapa, S. O. (2018). General Overviews on Applications of ELISA. An *Enzyme-linked Immunosorbent Assay (ELISA)* (pp. 19-29). Springer, Singapore.
- Ilaslan, K., Boyaci, I. H., and Topcu, A. (2015). Rapid analysis of glucose, fructose, and sucrose contents of commercial soft drinks using Raman spectroscopy. *Food Control* **48**, 56–61.
- Jaafarpour, M., Hatefi, M., Khani, A., and Khajavikhan, J. (2015). Comparative effect of cinnamon and Ibuprofen for treatment of primary dysmenorrhea: a randomized double-blind clinical trial. *Journal of clinical and diagnostic research: JCDR*, **9**(4), QC04.
- Jansson, N., Nilselfelt, A., Gellerstedt, M., Wennergren, M., Rossander-Hulthén, L., Powell, T. L., and Jansson, T. (2008). Maternal hormones linking maternal body mass index and dietary intake to birth weight. *The American journal of clinical nutrition*, **87**(6), 1743-1749.

- Jashni, H. K., Jahromi, H. K., Ranjbary, A. G., Jahromi, Z. K., and Kherameh, Z. K. (2016). Effects of aqueous extract from *Asparagus Officinalis* L. roots on hypothalamic-pituitary-gonadal axis hormone levels and the number of ovarian follicles in adult rats. *International Journal of Reproductive BioMedicine*, **14**(2), 75.
- Jebaliya, H., Patel, M., Jadeja, Y., Dabhi, B., and Shah, A. (2013). A Comparative Validation Study of Fluconazole by HPLC and UPLC with Forced Degradation Study. *Chromatography Research International*, **2013** (2013).
- Jenkins, A. L., Larsen, R. A., and Williams, T. B. (2005). Characterization of amino acids using Raman spectroscopy. *Spectrochimica Acta Part A: Molecular and Biomolecular Spectroscopy*, **61**(7), 1585-1594.
- Joo, D. S., Choi, D. J., and Park, H. (2000). The effects of data preprocessing in the determination of coagulant dosing rate. *Water Research*, **34**(13), 3295-3302.
- Kaaria, L. M., Oduma, J. A., Kaingu, C. K., Mutai, P. C., and Wafula, D. K. (2019). Effect of *Asparagus racemosus* on selected female reproductive parameters using the Wistar rat model. *Discovery Phytomedicine*, **6**(4), 199-204.
- Kanter, E. M., Majumder, S., Kanter, G. J., Woeste, E. M., and Mahadevan-Jansen, A. (2009). Effect of hormonal variation on Raman spectra for cervical disease detection. *American journal of obstetrics and gynecology*, **200**(5), 512-e1.
- Karimi Jashni, H., Kargar Jahromi, H., Ranjbary, A. G., Kargar Jahromi, Z., and Khabbaz Kherameh, Z. (2018). Effects of aqueous extract from *Asparagus Officinalis* L. roots on hypothalamic-pituitary-gonadal axis hormone levels and the number of ovarian follicles in adult rats. *Int. J. Reprod. Biomed.* **14**, 75–80.
- Khatun, S., Nara, S., Tripathi, V., Rangari, K., Chaube, S. K., Kariya, K. P., ... and Shrivastav, T. G. (2009). Development of ELISA for Measurement of Progesterone Employing 17- α -OH-P-HRP as Enzyme Label. *Journal of Immunoassay and Immunochemistry*®, **30**(2), 186-196.
- Kong, K., Kendall, C., Stone, N., and Notingher, I. (2015). Raman spectroscopy for medical diagnostics—From in-vitro biofluid assays to in-vivo cancer detection. *Advanced drug delivery reviews*, **89**, 121-134.
- Kudelski, A. (2008). Analytical applications of Raman spectroscopy. *Talanta*, **76**(1), 1-8.

Kumar, A., and Singh, A. (2001). Enhancement of conception rate by EveCare after ovulation induction by clomiphene citrate followed by intrauterine insemination. *Advances in Obstetrics and Gynecology*, **1**(5), 283-5.

Kumar, R., Malik, A. K., Kabir, A., and Furton, K. G. (2014). Efficient analysis of selected estrogens using fabric phase sorptive extraction and high-performance liquid chromatography-fluorescence detection. *Journal of Chromatography A*, **1359**, 16-25.

Lee, L. C., Liong, C. Y., and Jemain, A. A. (2018). Partial least squares-discriminant analysis (PLS-DA) for classification of high-dimensional (HD) data: a review of contemporary practice strategies and knowledge gaps. *Analyst*, **143**(15), 3526-3539.

Li, J., Wang, C., Kang, H., Shao, L., Hu, L., Xiao, R., ... and Gu, B. (2018). Label-free identification carbapenem-resistant *Escherichia coli* based on surface-enhanced resonance Raman scattering. *RSC advances*, **8**(9), 4761-4765.

Li, P., Hu, B., He, M., and Chen, B. (2014). Ion pair hollow fiber liquid-liquid-liquid microextraction combined with capillary electrophoresis-ultraviolet detection for the determination of thyroid hormones in human serum. *Journal of Chromatography A*, **1356**, 23-31.

Li, Y., Du, G., Cai, W., and Shao, X. (2011). Classification and quantitative analysis of Azithromycin tablets by Raman spectroscopy and chemometrics. *American Journal of Analytical Chemistry*, **2**(02), 135.

Lightfoot, J. T. (2008). Sex hormones' regulation of rodent physical activity: a review. *International journal of biological sciences*, **4**(3), 126.

Massarini, E., Wästerby, P., Landström, L., Lejon, C., Beck, O., and Ola, P. (2015). Sensors and Actuators B: Chemical Methodologies for assessment of limit of detection and limit of identification using surface-enhanced Raman spectroscopy. *Sens. Actuators B Chem.* **207**, 437-446.

Mendonça, M. C. P., Soares, E. S., de Jesus, M. B., Ceragioli, H. J., Ferreira, M. S., Catharino, R. R., and da Cruz-Höfling, M. A. (2015). Reduced graphene oxide induces transient blood-brain barrier opening: an in vivo study. *Journal of nanobiotechnology*, **13**(1), 1-13.

Minaeva, V. A., Minaev, B. F., and Hovorun, D. N. (2008). Vibrational spectra of the steroid hormones, estradiol, and estriol, calculated by density functional theory. The role of low-frequency vibrations. *Ukr. Biokhim. Zh*, **80**(4), 82-95.

Moura, C. C., Tare, R. S., Oreffo, R. O., and Mahajan, S. (2016). Raman spectroscopy and coherent anti-Stokes Raman scattering imaging: prospective tools for monitoring skeletal cells and skeletal regeneration. *Journal of The Royal Society Interface*, **13**(118), 20160182.

Naveed, S., Ghayas, S., and Hameed, A. (2015). Hormonal Imbalance and Its Causes in Young Females. *J. Innov. Pharm. Biol. Sci.* **2**, 12–16.

Nelson, R. E., Grebe, S. K., O’Kane, D. J., and Singh, R. J. (2004). Liquid chromatography-tandem mass spectrometry assay for simultaneous measurement of estradiol and estrone in human plasma. *Clinical chemistry*, **50**(2), 373-384.

Otange, B. O., Birech, Z., Okonda, J., and Rop, R. (2017). Conductive silver paste smeared glass substrates for label-free Raman spectroscopic detection of HIV-1 and HIV-1 p24 antigen in blood plasma. *Analytical and bioanalytical chemistry*, **409**(12), 3253-3259.

Patil, S. R., Yadav, N., Mousa, M. A., Alzwiri, A., Kassab, M., Sahu, R., and Chuggani, S. (2015). Role of female reproductive hormones estrogen and progesterone in temporomandibular disorder in female patients. *Journal of Oral Research and Review*, **7**(2), 41.

Paul, L. C., Suman, A. Al, and Sultan, N. (2013). Methodological Analysis of Principal Component Analysis (PCA) Method. *IJCEM Int. J. Comput. Eng. Manag. ISSN* **16**, 2230–7893.

Potcoava, M. C., Futia, G. L., Aughenbaugh, J., Schlaepfer, I. R., and Gibson, E. A. (2014). Raman and coherent anti-Stokes Raman scattering microscopy studies of changes in lipid content and composition in hormone-treated breast and prostate cancer cells. *Journal of biomedical optics*, **19**(11), 111605.

Quabis, S., Dorn, R., Eberler, M., Glöckl, O., and Leuchs, G. (2000). Focusing light to a tighter spot. *Optics Communications*, **179**(1-6), 1-7.

Ramdhani, R. A., Khojandi, A., Shylo, O., and Kopell, B. H. (2018). Optimizing clinical assessments in Parkinson's disease through the use of wearable sensors and data-driven modeling. *Frontiers in computational neuroscience*, **12**, 72.

Raquel, I. R. M., Malkin, A., and Lyng, F. M. (2015a). Current advances in the application of Raman spectroscopy for molecular diagnosis of cervical cancer. *BioMed research international*, 2015.

Reddy, P. R., and Raju, N. (2012). Gel-electrophoresis and its applications. *Gel Electrophoresis-Principles and basics, InTech*, 2, 15-32.

Ressom, H. W., Varghese, R. S., Abdel-Hamid, M., Eissa, S. A. L., Saha, D., Goldman, L., ... and Goldman, R. (2005). Analysis of mass spectral serum profiles for biomarker selection. *Bioinformatics*, 21(21), 4039-4045.

Robertson, D. M., Pruyers, E., Stephenson, T., Pettersson, K., Morton, S., and McLachlan, R. I. (2001). Sensitive LH and FSH assays for monitoring low serum levels in men undergoing steroidal contraception. *Clinical endocrinology*, 55(3), 331-339.

Sato-Berrú, R. Y., Medina-Valtierra, J., Medina-Gutiérrez, C., and Frausto-Reyes, C. (2004). Quantitative NIR–Raman analysis of methyl-parathion pesticide microdroplets on aluminum substrates. *Spectrochimica Acta Part A: Molecular and Biomolecular Spectroscopy*, 60(10), 2231-2234.

Schotsmans, E. M., Wilson, A. S., Brettell, R., Munshi, T., and Edwards, H. G. (2014). Raman spectroscopy is a non-destructive screening technique for studying white substances from archaeological and forensic burial contexts. *Journal of Raman Spectroscopy*, 45(11-12), 1301-1308.

Sengupta, P. (2013). The laboratory rat: relating its age with humans. *International journal of preventive medicine*, 4(6), 624.

Shah, R. B., Tawakkul, M. A., and Khan, M. A. (2007). Process analytical technology: chemometric analysis of Raman and near infra-red spectroscopic data for predicting physical properties of extended-release matrix tablets. *Journal of Pharmaceutical Sciences*, 96(5), 1356-1365.

Shao, B., Zhao, R., Meng, J., Xue, Y., Wu, G., Hu, J., and Tu, X. (2005). Simultaneous determination of residual hormonal chemicals in meat, kidney, liver tissues, and milk by liquid chromatography-tandem mass spectrometry. *Analytica Chimica Acta*, 548(1-2), 41-50.

Sharma, K. (2011). Asparagus racemosus (Shatavari): A versatile female tonic. *Int. J. Pharm. Biol. ...* 171, 142–51.

- Sitruk-Ware, R., and El-Etr, M. (2013). Progesterone and related progestins: potential new health benefits. *Climacteric*, *16*(sup1), 69-78.
- Stellato, R. K., Feldman, H. A., Hamdy, O., Horton, E. S., and McKinlay, J. B. (2000). Testosterone, sex hormone-binding globulin, and the development of type 2 diabetes in middle-aged men: prospective results from the Massachusetts male aging study. *Diabetes care*, *23*(4), 490-494.
- Stöckle, R. M., Suh, Y. D., Deckert, V., and Zenobi, R. (2000). Nanoscale chemical analysis by tip-enhanced Raman spectroscopy. *Chemical Physics Letters*, *318*(1-3), 131-136.
- Strola, S. A., Baritoux, J. C., Schultz, E., Simon, A. C., Allier, C., Espagnon, I., ... and Dinten, J. M. (2014). Single bacteria identification by Raman spectroscopy. *Journal of biomedical optics*, *19*(11), 111610.
- Ullah, R., Khan, S., Farman, F., Bilal, M., Krafft, C., and Shahzad, S. (2019). Demonstrating the application of Raman spectroscopy together with a chemometric technique for screening of asthma disease. *Biomedical optics express*, *10*(2), 600-609.
- Vance, S., Zeidan, E., Henrich, V. C., and Sandros, M. G. (2016). Comparative analysis of human growth hormone in serum using SPRi, nano-SPRi, and ELISA assays. *JoVE (Journal of Visualized Experiments)*, *107*, e53508.
- Vargis, E., Byrd, T., Logan, Q., Khabele, D., and Mahadevan-Jansen, A. (2011). The sensitivity of Raman spectroscopy to normal patient variability. *J. Biomed. Opt.* *16*, 117004.
- Vargis, E., Webb, C. N., Paria, B. C., Bennett, K. A., Reese, J., Al-Hendy, A., and Mahadevan-Jansen, A. (2011, March). Detecting changes during pregnancy with Raman spectroscopy. In *Proceedings of the 2011 Biomedical Sciences and Engineering Conference: Image Informatics and Analytics in Biomedicine* (pp. 1-4). IEEE.
- Varmuza, K., and Filzmoser, P. (2016). *Introduction to multivariate statistical analysis in chemometrics*. CRC press.
- Vedad, J., Mojica, E. R. E., and Desamero, R. Z. (2018). Raman spectroscopic discrimination of estrogens. *Vibrational Spectroscopy*, *96*, 93-100.
- Vincent, K., and Tracey, I. (2008). Hormones and their interaction with the pain experience. *Reviews in Pain*, *2*(2), 20-24.

Wahadoszamen, M., Rahaman, A., Hoque, N. M., I Talukder, A., Abedin, K. M., and Haider, A. F. M. (2015). Laser Raman spectroscopy with different excitation sources and extension to surface-enhanced Raman spectroscopy. *Journal of Spectroscopy*, 2015.

Webb, A. L., Hibbard, P. B., and O'Gorman, R. (2018). Natural variation in female reproductive hormones does not affect contrast sensitivity. *Royal Society open science*, **5**(2), 171566.

Westwood, F. R. (2008). The female rat reproductive cycle: a practical histological guide to staging. *Toxicologic pathology*, **36**(3), 375-384.

Wu, W., and Massart, D. L. (1996). Artificial neural networks in classification of NIR spectral data: Selection of the input. *Chemometrics and Intelligent Laboratory Systems*, **35**(1), 127-135.

Xu, S., Wang, D., Zhou, D., Lin, Y., Che, L., Fang, Z., and Wu, D. (2015). Reproductive Hormone and Transcriptomic Responses of Pituitary Tissue in Anestrus Gilts Induced by Nutrient Restriction. *PloS one*, **10**(11).

Zavaleta, C. L., Smith, B. R., Walton, I., Doering, W., Davis, G., Shojaei, B., ... and Gambhir, S. S. (2009). Multiplexed imaging of surface-enhanced Raman scattering nanotags in living mice using noninvasive Raman spectroscopy. *Proceedings of the National Academy of Sciences*, **106**(32), 13511-13516.

Zerihun, S. (2017). Research article home built lasing action: a review on nitrogen laser. *International Journal of current research*, **9**(7), 53952-53957.

Zhang, Y., Zhou, J. L., and Ning, B. (2007). Photodegradation of estrone and 17 β -estradiol in water. *Water Research*, **41**(1), 19-26.

Zhang, X., Young, M. A., Lyandres, O., and Van Duyne, R. P. (2005). Rapid detection of an anthrax biomarker by surface-enhanced Raman spectroscopy. *Journal of the American Chemical Society*, **127**(12), 4484-4489.

Zhelavskaya, I. S., Shprits, Y. Y., and Spasojevic, M. (2018). Reconstruction of plasma electron density from satellite measurements via artificial neural networks. In *Machine learning techniques for space weather*, 301-327. Elsevier.

APPENDICIES

APPENDIX 1: PCA Script in R

```
# loading the libraries

library(ChemoSpecUtils)

library(ChemoSpec)

library(knitr)

library(R.utils)

library(utils)

library(devtools)

library(pls)

# Reading a matrix data file stored in the working directory

spec <- matrix2SpectraObject(gr.crit=c("est","fsh", "lh", "pro"), gr.cols = c( "red", "blue",
"green" ,"black"),

                             freq.unit = "Raman shift (/cm)",

                             int.unit = "intensity",

                             descrip = "STANDARD Study",

                             in.file = "standhormeannn.csv",

                             out.file = "hormones", chk = TRUE, sep = ",", dec = ".")

# Summarizing the data

sumSpectra(spec)

#remove bad sample

out<-removeSample (spec, rem.sam = "T1rc_17")

#baseline using polynomial fit

spec2<-baselineSpectra (spec, int = FALSE, method = "modpolyfit", retC = TRUE)

spec3<-normSpectra(spec1)

pca <- r_pcaSpectra (spec3,

                    choice = "noscale")

plotScree(pca)
```

```

plotScores(spec3, pca,
  main = "STANDARDHORMONES pca",
  pcs = c(1,2),
  ellipse = "cls",
  tol = 0.1)
plotScores (spec3, pca,
  main = "STANDARDHORMONES pca",
  pcs = c(1,3),
  ellipse = "cls",
  tol = 0.1)
plotScores (spec3, pca,
  main = "STANDARDHORMONES pca",
  pcs = c(2,3),
  ellipse = "cls",
  tol = 0.1)
#potential outliers
diagnostics<-pcaDiag(spec3, pca, pcs = 2, plot = c("OD","SD"))
#number of pcs measured
plotLoadings(spec3, pca, loads = c(1,3), ref = 37)
plotScores3D(spec3, pca, ellipse=TRUE, tol = 0.01)

```

APPENDIX 2: ARTIFICIAL NEURAL NETWORK SCRIPT IN R

```
#loading libraries

library(neuralnet)

library(devtools)

library(caret)

library(ggplot2)

library(boot)

library(plyr)

#reading data

mydata=read.csv('pro.csv',sep="," ,header=TRUE)

mydata

attach(mydata)

names(mydata)

#data partitioning

indexs <- sample(1:nrow(mydata), round(0.70*nrow(mydata)))

datatrain <- mydata[indexs, ]

datatest <- mydata[-indexs, ]

#data normalizing

maxValue <- apply(mydata, 2, max)

minValue <- apply(mydata, 2, min)

data <- as.data.frame(scale(mydata,center=minValue,

                           scale = maxValue-minValue))

#data partitioning after normalisation

set.seed(1)

index = sample(1:nrow(data),round(0.70*nrow(data)))

train_data <- data[index,]
```

```

test_data <- data[-index,]

#ploting the model

model=neuralnet(CONC~.,data, hidden=18, act.fct = "logistic", threshold = 0.01, algorithm =
"rprop+", err.fct = "sse", linear.output = T)

model$net.result

plot(model)

#predicting the model

predcal_data = compute(model,train_data[,c(1:18)])

predcal_data$net.result

pred_trainNN = predcal_data$net.result

#rms(error of prediction obtained)

RMSEcal_model = (sum((train_data$CONC-pred_trainNN)^2)/nrow(train_data)) ^ 0.5

#Rsquared_model = 1 - sum((datatest$conc-pred_testNN)^2)/sum(datatest$conc-
(sum(datatest$conc)/nrow(datatest))^2)

Rsquaredcal_model = 1 - sum((train_data$CONC-pred_trainNN)^2)/sum(train_data$CONC-
(sum(train_data$CONC)/nrow(train_data))^2)

#standard deviation

S_model=(sum(pred_trainNN-
(sum(pred_trainNN)/nrow(train_data)))^2)/nrow(train_data)^0.5

#Mean absolute error obtained

MAEcal_model = (sum((train_data$CONC-pred_trainNN)^2)^0.5 / nrow(train_data))

#ANN model using caret

#loading libraries

library(caret)

#read input

set.seed(1)

input_data <- read.csv("pro.csv",
                      sep=',', header = T)

n <- nrow(input_data)

```



```

#normalisation of data

normalize <- function(x) {x <- as.numeric(x) return((x - min(x)) / (max(x) - min(x)))}

normalisedData <- as.data.frame(apply(input_data, 2, normalize))

#number of fold (if k=n, leave one out cross validation)

k <- n

folds <- createFolds(1:n, k, list = TRUE,returnTrain = FALSE)

predValue <- NULL

nn_result <- NULL

for(fold in folds){trainNN <- normalisedData[-fold, ]

  testNN <- normalisedData[fold, ]

  form <- as.formula("CONC~.")

  NeuralNet <- neuralnet(form, trainNN, hidden = 18, act.fct = "logistic", threshold = 0.01,
    stepmax = 1e+05, rep = 1, startweights = NULL,
    learningrate.limit = NULL,
    learningrate.factor = list(minus = 0.5, plus = 1.2),
    learningrate = NULL, lifesign = "none",
    lifesign.step = 1000, algorithm = "rprop+",
    err.fct = "sse", linear.output = TRUE, exclude = NULL,
    constant.weights = NULL, likelihood = FALSE)}

plot(NeuralNet)

pred_test <- compute(NeuralNet, testNN)

pred_test$net.result

actual_pred = data.frame(pre = pred_test$net.result,
  actual = testNN$CONC)

plot(actual_pred, main="prediction vs actual", col='blue' , xlab="Actual", ylab="Predicted",
pch=15, type="p")

abline(0,1, col="black")

#Calculating RMSE

```

```

predict_testNN = (pred_test$net.result)

rms = function(x) 1 - (x/(nrow(trainNN) - 1)*var(trainNN$conc))

#rms(error obtained)

RMSError = (sum((testNN$conc-predict_testNN)^2) / nrow(testNN)) ^ 0.5

#Saving the model

save(model, file = "model")

#loading the model

load(file = "model")

#read input

set.seed(1)

indata <- read.csv("pro.csv", sep=',', header = T)

n <- nrow(indata)

normalize <- function(x) {
  x <- as.numeric(x)
  return((x - min(x)) / (max(x) - min(x)))}

normalisedinData <- as.data.frame(apply(indata, 2, normalize))

val_data_model_pro <- compute(model, normalisedinData[,c(2:18)])

val_data_model_pro$net.result

denormalizedval_data_model_pro<-val_data_model_pro$net.result*
(max(input_data$CONC) - min(input_data$CONC)) + min(input_data$CONC)

denormalizedval_data_model_pro

#predicting group1_data

set.seed(1)

group1 <- read.csv("group1_pro.csv", sep=',', header = T)

n <- nrow(indata)

normalize <- function(x) {
  x <- as.numeric(x)
  return((x - min(x)) / (max(x) - min(x)))}

```

```
group1_pro <- as.data.frame(apply(group1, 2, normalize))  
val_data_model_group1_prp <- compute(model,  
                                     group1_pro[,c(2:30)])  
val_data_model_group1_pro$net.result  
denormalizedval_data_model_group1_pro<-val_data_model_group1_pro$net.result*  
(max(input_data$conc) - min(input_data$conc)) + min(input_data$conc)  
denormalizedval_data_model_group1_pro  
tmp1 <- cbind(group1_pro$conc, denormalizedval_data_model_group1_pro)  
colnames(tmp1) <- c("group", "conc")  
write.csv(tmp1,"group1predconc.csv")
```

APPENDIX 3: Raman Spectroscopy set up at the Department of Physics, University of Nairobi



APPLICATION OF RAMAN SPECTROSCOPY IN COMPARATIVE STUDY ON THE INFLUENCE OF IBUPROFEN AND *Asparagus racemosus* (HERBAL EXTRACT) ON FEMALE REPRODUCTIVE HORMONES IN WISTAR RATS

ORIGINALITY REPORT

Checked and approved Dr. Z. Bi

on 17/11/2020

14%

SIMILARITY INDEX

8%

INTERNET SOURCES

8%

PUBLICATIONS

5%

STUDENT PAPERS

25/11/2020

PRIMARY SOURCES

1	Submitted to University of Nairobi Student Paper	3%
2	worldwidescience.org Internet Source	1%
3	www.jri.ir Internet Source	1%
4	hdl.handle.net Internet Source	<1%
5	Zephania Birech, Peter W. Mwangi, Prabjot K. Sehmi, Nelly M. Nyaga. " Application of Raman spectroscopy in comparative study of antiobesity influence of oxytocin and freeze-dried extracts of () in Sprague Dawley rats ", Journal of Raman Spectroscopy, 2019 Publication	<1%
6	"Handbook of Graphene", Wiley, 2019 Publication	<1%

DEAN
SCHOOL OF PHYSICAL SCIENCES
UNIVERSITY OF NAIROBI

SI is within
acceptable limit
25/11/2020